DESY HERA 84-07

April 1984

# PARTICLE TRACKING FOR HERA

A. Wrulich

Invited paper presented at the DPF Workshop 'Accelerator Physics Issues for an SSC', University of Michigan, Ann Arbor, December 12-17, 1983

Contents

## 1. Introduction

The existence of a good linear optics is no guarantee for a proper functioning of an accelerator. Deviations from the linearized equations of transverse motion even for a single particle may arise due to magnetic fields of higher order, which are either introduced artificially, as for instance sextupoles to compensate the natural chromaticity, or undesired deviations from linear fields due to finite magnet size, coil geometry in superconducting magnets, fabrication errors, etc.

Including general fields, the transverse motion of a single particle in the nonlinear lattice can be expressed by the following equations:

$$\frac{d^2x}{ds^2} + K_x(s)\, x = \frac{e}{p_o} B_z\,(z,x,s) \qquad (1a)$$

$$\frac{d^2z}{ds^2} + K_z(s)\, z = -\frac{e}{p_o} B_x(z,x,s) \qquad (1b)$$

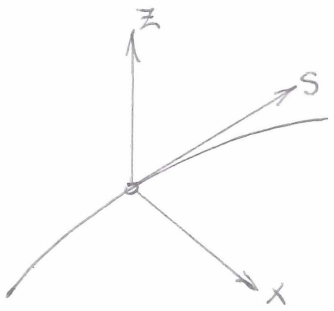


$x,z$ ..... horizontal and vertical displacement
$s$ ..... longitudinal coordinate
$K_x, K_z$ .... focusing strengths including weak and edge focusing
$B_x, B_z$ .... transverse components of the additional magnetic field ($B_s = 0$)
$p_o$ ..... momentum of the particle

It is practical to use a multipole expansion for the analytical description of the field, which in complex notation has the following simple form:

$$B_z + i\,B_x = \sum_{n=1}^{\infty} (b_n + i a_n)(x+iz)^{n-1} \qquad (2)$$

with n corresponding to a 2n-pole

$b_n$, $a_n$ ... normal and skew multipole coefficients (a normal multipole does not couple an initial purely horizontal motion in the vertical plane)

Comparing the multipole ansatz with a Taylor expansion, the multipole coefficients may be expressed as derivatives of the magnetic field components

$$a_n = \frac{1}{n!} \cdot \frac{\partial^n B_x}{\partial x^n} \qquad (3a)$$

$$b_n = \frac{1}{n!} \cdot \frac{\partial^n B_z}{\partial x^n} \qquad (3b)$$

$$(\vec{\nabla}\vec{B} = 0,\ \vec{\nabla} \times \vec{B} = 0)$$

Since in general there exist no analytical solutions for these equations anymore, a computer simulation must be performed to investigate the particle dynamic in the presence of arbitrary field distortions.

Doing this, the equations of motions are first solved piecewise for each element. For linear elements (with focusing strength and radius of curvature constant) the solutions and their derivatives may be written in matrix form and the final coordinates at the end of the magnet may be related to the initial coordinates by the following linear transformation:

$$\begin{bmatrix} x \\ x' \end{bmatrix}_f = \begin{bmatrix} C & S \\ C' & S' \end{bmatrix} \begin{bmatrix} x \\ x' \end{bmatrix}_i \qquad (4)$$

C, S ... cosinelike and sinelike solutions of equations of motion

$'$ ... $\frac{d}{ds}$

$x_f$, $x_i$ ... final and initial coordinate vector

To make the nonlinear equation solvable, a thin magnet representation is used, that means the integrated effect is concentrated in a 'thin magnet' element with zero length:

$$x'' = -\frac{e}{p_o}\,\delta(s)\int_{-1/2}^{+1/2} B(z,x,s)\,ds \qquad (5)$$

If the nonlinear field cannot be represented by a single thin magnet, one should divide it into sufficiently small sections, so that each of the sections is regarded as 'thin magnet'.

The following calculations are restricted on investigating the influence of transverse magnetic multipole fields on particle motion.

Collective effects are not taken into account, as for instance the beam-beam effect, fields induced in cavities and walls, etc.

## 2. Simulation program RACETRACK /1/

Tracking in performed by transforming an ensemble of particles with different initial coordinates through the structure, as sketched in the following picture:

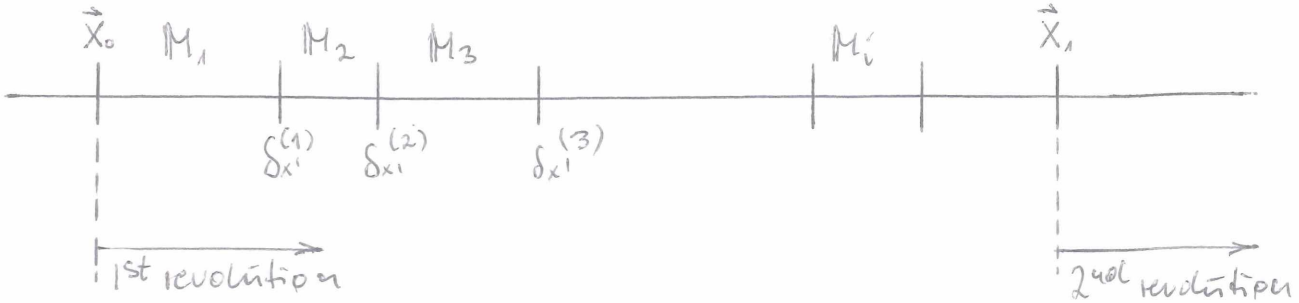


$M_i$ ... linear transformations
$x'$ ... deflection due to nonlinear elements

The linear elements between two nonlinear insertions are composed into a single unit represented by its transformation matrix only. Nonlinear elements are treated in thin magnet approximation.

An important question is, how to choose the initial distribution, for getting a maximum of information with a minimum of computer time.

Since the linear dimensions of the beam vary according to the focusing structure, the linear beam size at the starting point must first be found, that means the optical beta and alfa values must be calculated. Then the initial trajectory coordinates lying on phase ellipses with constant betatron amplitude are distributed uniformly on the ellipses of both planes.

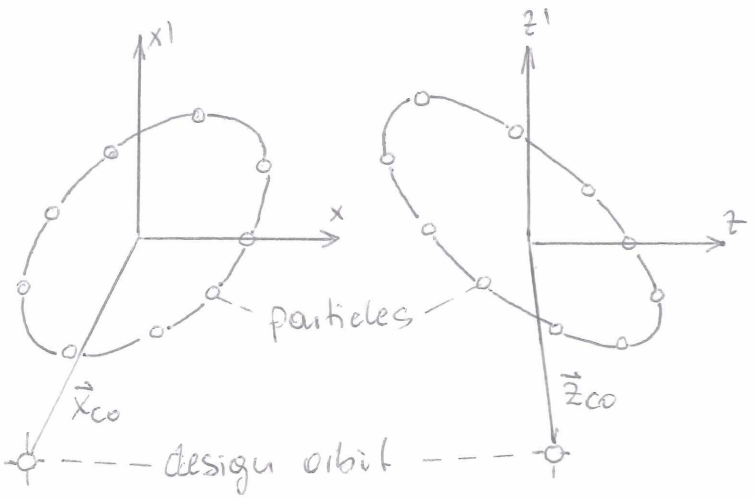


Each trajectory vector of the horizontal plane is combined with every vector of the vertical plane to give the total number of initial trajectories for one pair of horizontal and vertical amplitudes.

For the tracking, the maximum stable amplitude A or emittance $\varepsilon$, which is proportional to the areas of the ellipses, is taken as a quality factor. If dipole errors are included, or in the off energy case the ellipses are shifted in phase space by the closed orbit vectors $x_{co}$ and $z_{co}$. Therefore

first the closed orbit must be found in the presence of all nonlinear elements and then the optics with linearized fields at this orbit must be calculated.

Regarding the initial coupling between horizontal and vertical motion described by the emittance ratio, the situation is different in the electron case as compared to protons.

For electrons the equilibrium between quantum excitation and damping gives a gaussian particle distribution. For horizontal and vertical displacements x, z and their derivatives x', z' there is a four-dimensional gaussian distribution with standard deviations.

$$\begin{bmatrix} \sigma_x \\ \sigma_{x'} \end{bmatrix} = \sqrt{\varepsilon_x} \sqrt{\frac{\beta_x}{\gamma_x}} \quad , \quad \begin{bmatrix} \sigma_z \\ \sigma_{z'} \end{bmatrix} = \sqrt{\varepsilon_z} \sqrt{\frac{\beta_z}{\gamma_z}}$$

Since the emittance is produced by dispersion in bending magnets, the vertical emittance which is due to spurious dispersion (and some other usually small coupling mechanism) is much smaller than the horizontal emittance. Secondly the emittance ratio is constant for particles on hyperspheres with constant particle density, and scraping a beam along these hyperspheres gives the same reduction in lifetime.
Following this restriction, the initial amplitudes should be related as shown in this graph:

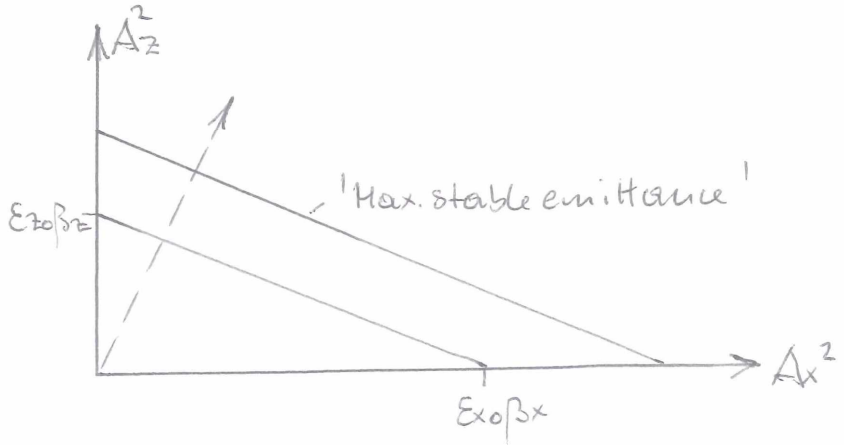


$$A_x = \sqrt{\varepsilon_x \beta_x} \cos\delta \qquad K = \frac{z_0}{x_0} = \frac{\varepsilon_z}{\varepsilon_x} = \text{const.}$$

$$A_z = \sqrt{\varepsilon_z \beta_z} \sin\delta \qquad \delta \ldots \text{ distribution parameter}$$

In terms of oscillation amplitudes the relation is quadratic

$$\frac{Ax^2}{\beta_x} + \frac{Az^2}{K\beta_z} = \varepsilon_x$$

and we call it an elliptical distribution. Following this picture, the maximum stable emittance $\varepsilon_x$ corresponds to the line with maximum distance from the origin. The actual shape of the stability boundary is of minor interest.

In proton accelerators the emittance ratio is usually between 0.5 and 1.0 and given by the injection procedure. In principle one can fill the whole stable acceptance with protons, thus the entire stability boundary is of interest.

Demonstration examples for proton calculations are given in Fig's 1 and 2. They are calculations for ACOL, the Antiproton Collector which is planned at CERN /2/. The nonlinear stability limit is drawn for 3 different energies. In Fig. 1 no aperture limitation was introduced. Therefore these curves correspond to boundaries given by fields only. In Fig. 2 the physical aperture limitation has been added.

Since the calculation of the entire boundary shape is very time consuming, one can restrict oneself to calculate the maximum stable amplitude with constant initial emittance ratio along the diagonal of the linear beam size as indicated in Fig. 2.

Once the amplitude distribution is chosen, the tracking will be performed by stepwise decreasing the amplitude to find the maximum stable value. An ensemble of particles is found to be stable, if all particles over all revolutions remain within the physical aperture. The aperture is represented in the program by aperture limiting insertions which can be placed at any point in the structure and may also have different aperture values. Thus the actual shape of the vacuum chamber can be introduced.

The aperture boundaries may be chosen as either -

rectangular $\quad x_i < Ap_x \wedge z_i < Ap_z$

or elliptical $\quad \left(\frac{x_i}{Ap_x}\right)^2 + \left(\frac{z_i}{Ap_z}\right)^2 < 1$

$x_i$, $z_i$ .... transverse particle coordinates
$Ap_x$, $Ap_z$ .. half apertures

To vary optical parameters, the following tasks may be activated in RACETRACK by introducing an additional switch data block in the input stream:

tune variation: the tune may be adjusted to desired values by changing two quadrupole families. This is important for exploring the stability range in the tune diagram around a suitable working point.

chromaticity adjustment: the chromaticities can automatically be adjusted to zero or any other value by tuning two sextupole families.

closed orbit distortion: positions of dipole errors and orbit displacement monitors may be defined. At the dipole positions a random set of errors can be introduced and scaled in strength to give desired rms orbit displacements measured at the monitor positions.

orbit correction: since the harmonic content of a so produced orbit is different from a corrected orbit (the fundamental harmonic is usually large), orbit errors produced in that way may also be corrected by using correction routines.

linear optics: the linear optics may be calculated, which is very helpful for input control and error detection.

Another possible feature is the introduction of energy variations according to the actual synchrotron oscillations. Cavities may be introduced aroung the circumference. Of course this operation needs more computer time, since

after each energy change the energy dependent linear transformations must be recalculated. Also, one needs more revolutions to see an influence of energy oscillations since the synchrotron frequency is much less than the revolution frequency. For large energy amplitudes near the boundaries (in which we are interested) the synchrotron frequency is even further reduced. Approaching the separatrix of the longitudinal motion, it is coming down to zero. Therefore in most cases one prefers to look for the stable amplitude at different constant energies within the energy spread of the beam. All calculations presented in this report are made for constant energy deviation.

But at least it can qualitatively be shown how the picture of nonlinear dynamics is changed if synchrotron oscillations are introduced in addition. First of all satellite resonances are excited. Apart from linear and nonlinear chromaticity there are two single particle coupling mechanisms between transversal and longitudinal motion.

1. A dispersion at the cavity position. The mechanism is sketched in the following picture:

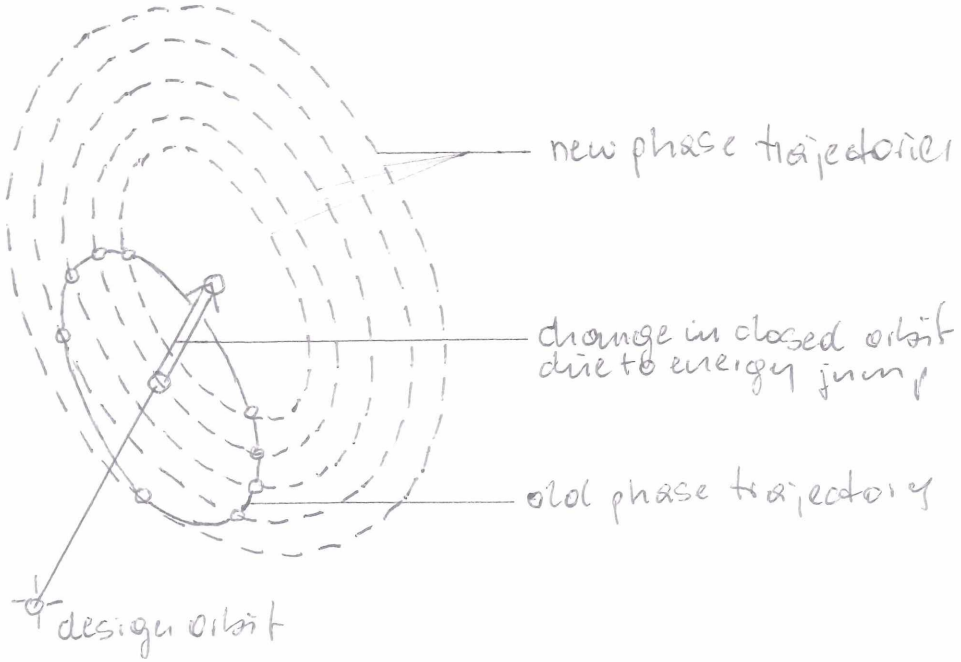

If the energy is changed, the corresponding closed orbit is changed. Since the particle coordinates are not changed, trajectories going around this new closed orbit have partly increased amplitudes. If the resonance condition is fulfilled, i.e.

$$\delta Q_\beta = n\, Q_s$$

$\delta Q_\beta$ ... fractional part of betatron tune
$Q_s$ ... synchrotron tune
n ..... integer

the particle becomes unstable.

2. Energy dependence of beta and alfa value at the cavity position:

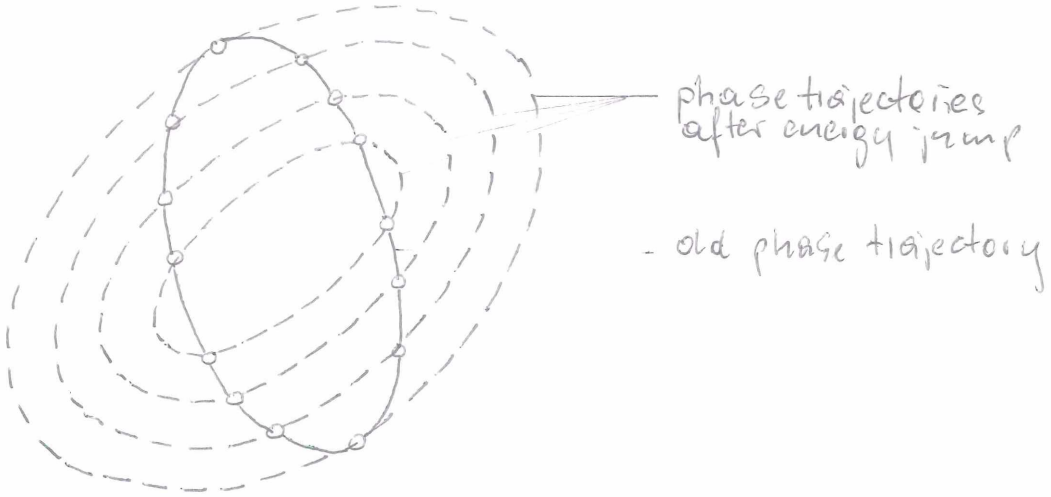


If the energy is changed, the shape of the phase trajectories is changed. Particles following the new phase ellipse have partly increased amplitudes. Again there is a growth in beam size if the resonance condition

$$\delta Q_\beta = n\, \frac{Q_s}{2}$$

is fulfilled.

Therefore synchrotron oscillations will cause beam blow-up as described by these two effects.

On the other hand, if there is a resonance in the range of the momentum-caused tune spread, synchrotron oscillations will average this effect and increase the stable amplitude at the resonance, at least as a short-time effect. Regarding long-time effects, synchrotron oscillations combined with resonances may produce diffusional beam growth.

## 3. HERA project /3/

HERA is a large electron proton colliding beam machine. 820 GeV protons collide with 30 GeV electrons in 4 interaction points. It is located on a site adjoining the DESY site (Fig. 3). The circumference of the ring is 6336 meters, which is just 2 3/4 times the length of PETRA.

The tunnel of HERA is lying 10 to 20 m under ground. Fig. 4 shows the cross section of the tunnel with the proton ring above the electron ring.

In the straight sections the proton ring is bent down to the level of the electron ring (Fig. 5). There is also a horizontal crossing angle of 20 mrad to avoid common elements. The total length of the straight section is 360 meters.

The arc is built of a FODO structure of 26 proton cells and 52 electron cells per quadrant (Fig. 6). The proton ring has 3 bending magnets per half cell and originally there was a correction package beside each quadrupole with also chromaticity correcting sextupoles included. In the new design sextupoles are introduced as additional windings in the magnets adjacent to the quadrupoles. In part 5 tracking results will be shown for both arrangements.

## 4. Nonlinear fields and their effects on particle motion

Nonlinear fields affecting the transverse single particle motion can be grouped into 2 parts:
First, since it is impossible to built an ideal magnet, there is always a certain multipole content in addition to the linear field, as for instance due to the finite magnet size, coil geometry in superconducting magnets and fabrication errors. Secondly, nonlinearities are also artificially introduced.

The most important nonlinearities artificially introduced are sextupoles. They are necessarely introduced to compensate the natural chromaticity,

$$\xi = \frac{\Delta Q}{\Delta p/p}$$

i.e. the linear part of tune variation with energy.

There are several reasons for compensating the chromaticity. First to avoid the head-tail instability which is dangerous in bunched beam accelerators with high intensity. Second to reduce the variation of tune with momentum. Otherwise during one synchrotron oscillation period the tune would cross resonance lines. Also sextupoles reduce the energy dependent beat of the beta functions, which has the effect that the aperture requirements are reduced and satellite resonances resulting from the variation of beta values with momentum are reduced.

But beside the desired effect of compensating the chromaticity,

$$\delta_{x'} = m\left(x + \frac{p}{p} D\right) = \underbrace{mx^2}_{\text{undesired nonlinear effect}} + \underbrace{\frac{\Delta p}{p}\,(2mD_x)}_{\xi\text{-correction}}\, x + \left(\frac{\Delta p}{p} D_x\right)^2$$

m ... integrated sextupole strength

$D_x$ .. horizontal dispersion

there is still the undesired nonlinear sextupole effect which will cause a blow-up of the initial betatron amplitude and must be investigated by tracking.

The simplest way to compensate the natural chromaticity would be to introduce a distribution of 2 sextupole families placed at all positions where the beta values are sufficiently decoupled and the dispersion is large enough. This might be a good solution if chromatical effects of higher order are small, that means if the energy spread of the beam is small.

If we use a 2-family distribution for the electron ring of HERA (old short cell design), the maximum stable initial amplitude behaves like shown in Fig. 7.

There the maximum stable horizontal amplitude is shown as a function of relative energy deviation. A rectangular initial particle distribution with constant emittance ratio of 0.1 was used for the tracking. The observation point is a focusing quadrupole in the normal cell. The lower curve corresponds to an optics which was matched for polarization without controlling the nonlinear acceptance. The dotted line corresponds to the beam size at 35 GeV. Even integer tunes corresponding to the lower curve are not suitable for structures with supersymmetry 4, since they are close to a half integer structure resonance which increases the higher order chromatical effects. After changing the integer part of tunes the acceptance could be increased as shown by the upper curve. But even there are strong resonance dips. For analysing these resonances one can look at the energy dependent variation of tune in the $Q_{x,z}$-plane (Fig. 8). At energy deviations corresponding to the dips in Fig. 7 , the tune has crossed 3rd integer resonance lines. It is evident that in this case we have to compensate the high order chromatical effects and introduce additional sextupole families.

## 5. Tracking Examples for the HERA Proton Ring /4,5/

For the proton ring, in addition to the chromaticity correcting sextupoles we have at low energies a large persistent current sextupole component in the superconducting magnets. For HERA the maximum injection energy is limited by the maximum energy of PETRA which will be used as injector for HERA.

For the injection energy of 40 GeV the chromaticities due to 'Persistent Current Sextupoles' (PCS) are changed from their natural values of

$$\xi_H = 64.5 \quad \text{to} \quad -297.0$$

$$\xi_V = 87.5 \quad \text{to} \quad +129.0$$

Fortunately the PCS are producing a positive vertical chromaticity; a large horizontal chromaticity is easier to compensate than a large vertical one.

To avoid problems we originally decided to compensate the PCS by a commonly powered coil. Only a random fluctuation of 10 % was taken into account as rms value for the tracking. Most tracking results shown in this report are based on this assumption.

Another large contribution affecting the nonlinear acceptance in the HERA proton ring is given by field errors in superconducting magnets. Since the field accuracy of superconducting magnets depends on mechanical tolerances of the coil, their field errors tend to be larger than in a conventional magnet. Typical peak values are:

$\pm 2.5 \cdot 10^{-4}$ for normal and skew quadrupoles

$\pm 6.0 \cdot 10^{-4}$ for normal sextupoles

$\pm 2.0 \cdot 10^{-4}$ for skew sextupoles and normal and skew multipoles up to 20-poles

They correspond to the FERMILAB specifications and are defined as the strengths of the multipole field at 1 inch distance from the center, divided by the normal bending strength. Apart from a systematic 14- and 18-pole, taken from our magnet calculations, 1/3 of the FERMILAB peak values was taken as rms value for the tracking.

To get a feeling how all these nonlinearities superimpose, first the acceptance as limited by normal chromaticity correcting sextupoles only was calculated. The integer parts of tune were matched to odd values. The effect of tune changes around a suitable working point is shown in Fig. 9. The variation of maximum stable initial amplitude (at the position of a horizontal focusing quadrupole in the normal cell) is shown as a function of small horizontal and vertical tune changes. The calculations are based on a cell with 90° phase advance and 0.5 initial emittance coupling. Common to all cuts in the tune plane is the decrease of stable amplitude for horizontal tunes approaching the $3^{rd}$ integer structure resonance. For the best choice of the tune, the nonlinear part of chromaticity is shown in Fig. 10. Since it is rather weak over the total energy spread of the beam of $\pm$ 1.5 %o, a 2-family compensation with an additional $3^{rd}$ integer resonance compensation will be sufficient.

For the optimum tunes of this rough optimization, the maximum stable amplitude was calculated for different constant energy deviations. The result is shown in Fig. 11. The number of revolutions used for the calculations was 100 in this case. Since the increase of stable revolutions near the stability limit is a very steep function, as shown in Fig. 12, this seems to be a reasonable number to investigate short time effects. You don't gain very much in accuracy of stable amplitude by going to more than 100 revolutions.

For the definition of the magnet aperture it is useful to know the nonlinear stability limit. In Fig. 13 the maximum stable amplitude is drawn as a function of free half aperture. The saturation level of this curve corresponds to the nonlinear acceptance. If you increase the aperture above this value, the maximum initial amplitude is not increased anymore and the particles are lost at the nonlinear field limit only. Two curves are drawn in Fig. 13., for 60° and 90° cell phase advance respectively. For 60° phase

advance the nonlinear limit is strongly increased. To understand this we can look at the sextupole strength necessary for a 2-family compensation:

$$m_F \left[ m^{-2} \right] = \frac{1}{\hat{D}} \left\{ \frac{1}{f} + \frac{4\pi |\xi_{IR}|}{N_e (\hat{\beta} - \check{\beta})} \right\} \quad m_D = m_F \frac{\hat{D}}{\check{D}}$$

$f$ .... focal length
$D$ .... cell dispersion
$N_e$ .... total no. of cells
$\xi_{IR}$ ... chromaticity of interaction regions
$\beta$ .... beta value in the cell

The sextupole strength is inversely proportional to the dispersion. The two added terms in the bracket correspond to chromaticities produced in the cell and in the interaction region. For decreasing phase advance the focal length is increasing (for constant cell length). Since the dispersion is increasing with the squared focal length and the cell beta beat proportional to the focal length, the sextupole strength is decreasing with the 3$^{rd}$ power of the focal length and the stability limit correspondingly increasing.

But if the aperture is fixed by other reasons, for instance by cost considerations, there is not much difference between 60° and 90° phase advance. In the off-energy case the situation is even worse for 60°. Due to the increased dispersion, the free aperture for off-energy particles is decreased.

In the next step multipoles were introduced in thin magnet approximation in the middle of each bending magnet. As already mentioned above, the average contribution of PCS (Persistent Current Sextupole) was compensated by a commonly powered coil in all dipoles. The statistical fluctuation of PCS was added quadratically to the geometrical sextupole error.

The multipole statistics was chosen in the following way: For an arbitrary set of random multipoles the tune optimization was performed as shown in Fig. 9, then for the optimum tune 20 different sets of multipole fluctuations were calculated (Fig. 14). One set out of the central part of the resulting distribution was used for the subsequent calculations. For

each run in Fig. 14 the tunes were always readjusted to their original values and dipole errors were scaled to generate a closed orbit distortion of 1 mm rms value measured at the positions of normal cell sextupoles.

For a random fluctuation set taken from the central region, the momentum dependence of the maximum stable initial amplitude is shown in Fig. 15. The single point at zero momentum deviation shows the result for multipoles only, i.e. the chromaticity correcting sextupoles are switched off. It demonstrates that the effects of sextupoles and multipoles on dynamical aperture are more or less comparable.

As already shown in Fig. 9, $3^{rd}$ integer resonances driven by sextupoles are quite dangerous even for tunes which are not close to the resonance.

The efficiency of a $3^{rd}$ integer resonance compensation was demonstrated by the program. Fig. 16 shows the stable amplitude vs. tune before compensation. As shown in Fig. 17, after compensation the stable amplitude is considerably increased /6/.

From magnet design calculations, rather strong systematic 14- and 18-poles were predicted. Fig. 18 shows the influence of systematic 14- and 18-poles on stable amplitude. All other nonlinearities are switched off. The solid lines correspond to calculations without aperture limitation; for the dotted line the nominal value of 30 mm half aperture was taken into account. In the range of interest around the HERA values, the amplitude reduction is close to the limit produced by all other nonlinearities (sextupoles + field errors), which is not acceptable. By introducing longitudinal spacers, the systematic 14- and 18-pole could be reduced by more than a factor of 10.

In connection with the PCS the question came up whether we really need the commonly powered coil to compensate the average contribution of PCS. If we compensate the chromaticity produced by PCS by the lattice sextupoles in the correction package only (see Fig. 6), the acceptance is further reduced as shown in Fig. 19. But in the meantime we decided to integrate the chromaticity correcting sextupoles in the bending magnets adjacent to the lattice quadrupoles. Changing to this new scheme, and at the same time

reducing the half aperture from 30 to 28 mm, we got a slightly reduced stable amplitude everywhere. But the compensation of PCS works very well in this new scheme, since 2 out of 3 magnets in the half cell are now locally compensated and for the 3$^{rd}$ one the compensation is closer to the source as compared to the previous scheme. In fact, within the accuracy of calculation no influence on stable amplitude was seen after correcting the PCS by the integrated lattice sextupoles (Fig. 20).

Fig. 21 shows the same result over a wider energy range. There is still place for increasing the energy spread to reduce the microwave instability. But the variation of tune with energy tends to become large, as shown in Fig. 22, and it might be necessary to introduce additional sextupole families to compensate the higher order chromatical effects.

The variation of stable amplitude with free aperture is shown for the new scheme in Fig. 23. It still looks quite satisfactory.

Another question in connection with the PCS was how the stability limit is affected if the filament diameter of the superconductors is increased. In that case the PCS is expected to increase proportional. Fig. 24 shows a diagram where the maximum stable amplitude (for zero momentum deviation) is drawn as a function of persistent current sextupole. There is a surprisingly small decrease of stable amplitude for growing systematic PCS as shown by the upper curve. The lower curve corresponds to a variation of PCS rms value.

So far all calculations with multipole errors included also dipole errors producing an orbit distortion of 1 mm rms. There are two effects coming from orbit distortions and influencing the stable amplitude. First the free aperture is reduced and secondly the multipole pattern is changed. In Fig. 25 the maximum stable initial amplitude is drawn for increasing orbit distortions with rms values equal in both planes. The tunes were always readjusted to their original values and the chromaticities were recompensated to zero. For values above 6 mm the beam size even for on-momentum particles is already being scraped. For off-momentum particles this might even be earlier the case.

Finally the critical question: "How many revolutions are necessary for realible results?" has been investigated. Fig.12 showed the pure sextupole case. There we had a rapid increase of stable revolutions moving away from the stability limit. The corresponding calculation with multipole errors, orbit errors and PCS compensation included, is shown in Fig. 26. Near the stability limit the particles seem to be very sensitive to resonances. But then again the number of stable revolutions rapidly increases when moving away from this region. Therefore, when tracking only 100 revolutions as compared to 30000 revolutions there is an uncertainty in the resulting amplitude which might be in the range of 1.5 mm.

## 6. References

/1/ A. Wrulich, "RACETRACK a Computer Code for the Simulation of Nonlinear Particle Motion in Accelerators", DESY 84/26

/2/ A. Wrulich, "Tracking Results for the AC Ring", CERN PS/AA/AC-23

/3/ HERA Proposal, ECFA 80/42 and DESY HERA 80/01, March 1980

/4/ A. Wrulich, "Aperture Limitations in the HERA Proton Ring due to Nonlinear Fields", DESY HERA 82/04, April 1982

/5/ A. Wrulich, "Tracking Studies in HERA", DESY HERA 82/07, June 1982

/6/ F. Schmidt, "Resonanzuntersuchungen bei HERA", DESY HERA 83/29, Dezember 1983

Fig. 1: ACOL (Antiproton COLlector)
Maximum stable amplitude, without aperture limitations (Optics AC83.08)

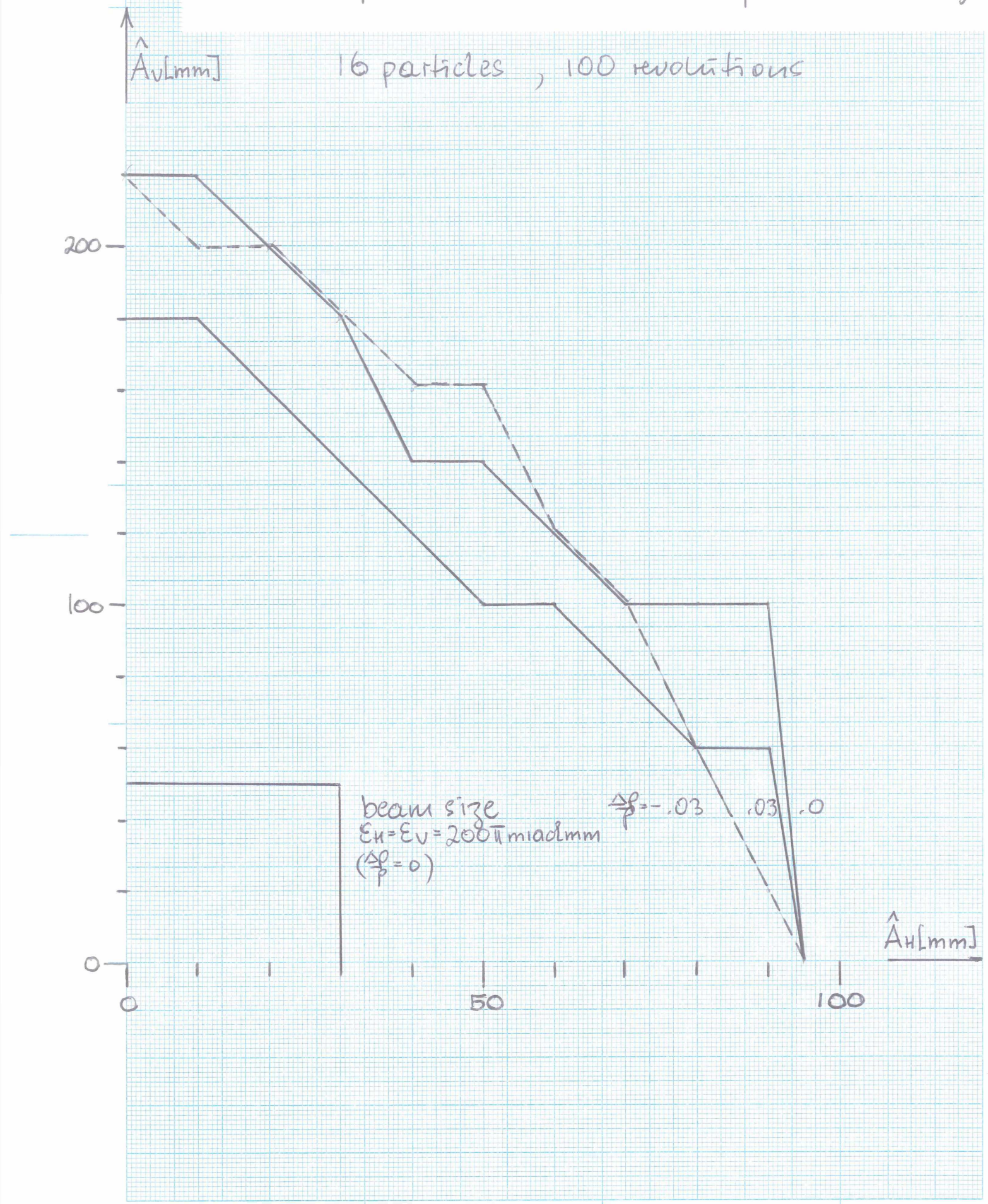

Fig. 2: ACOL
Maximum stable amplitude, with aperture limitations (Optics AC 83.08)

16 particles, 100 revolutions

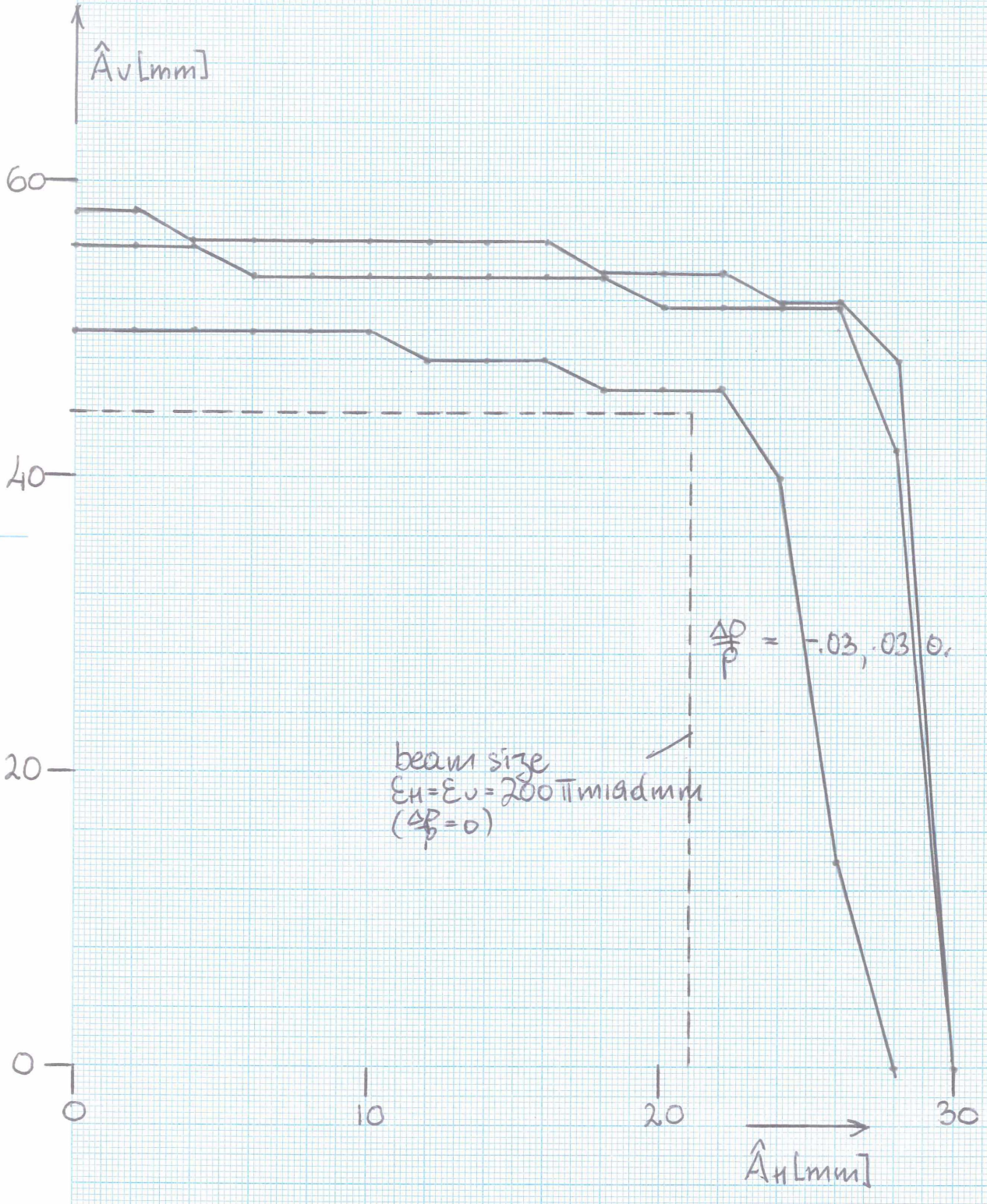


Fig 3: The layout of HERA

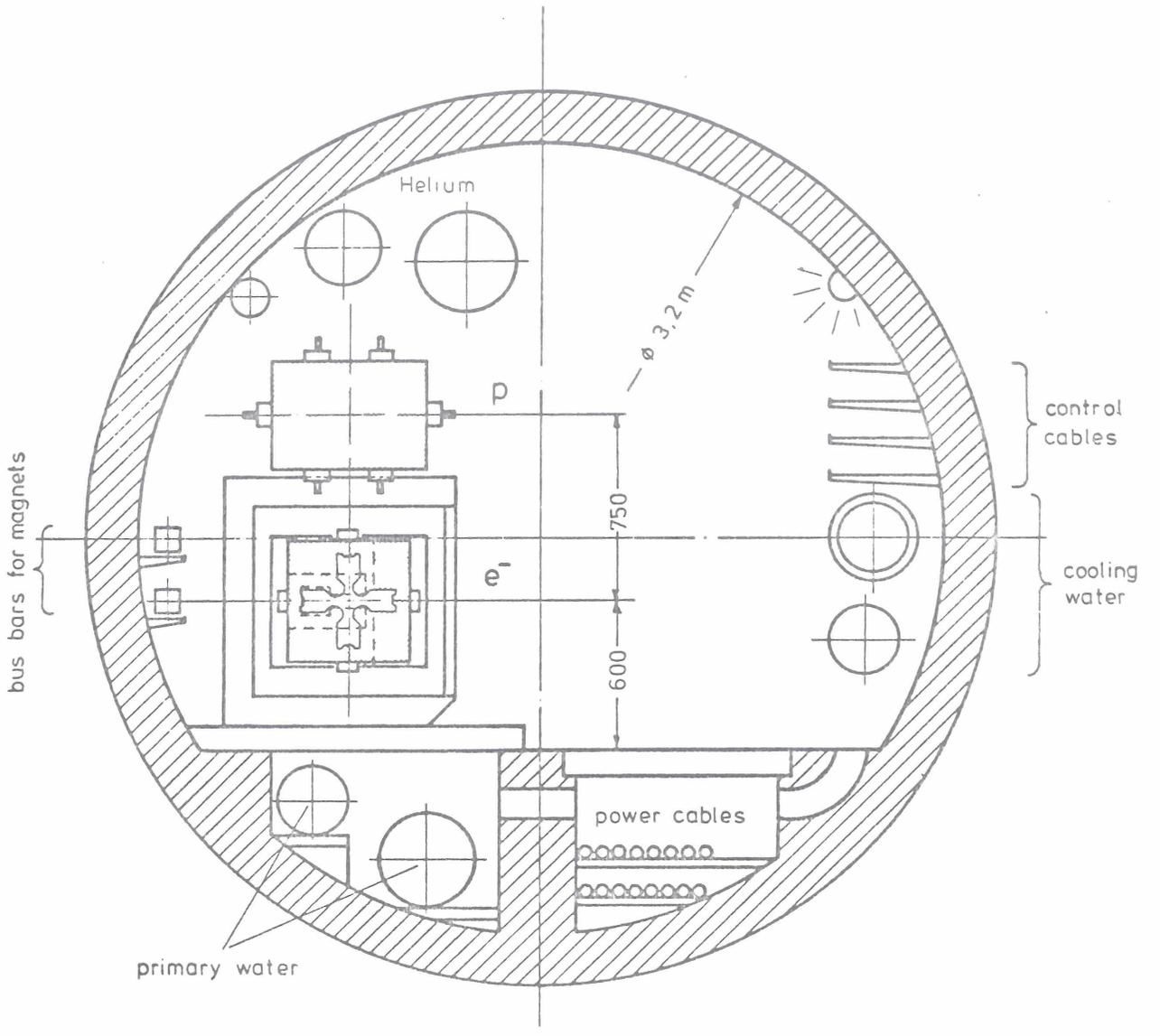


Fig. 4: Cross section of the HERA-tunnel in the arc

Fig. 6: Lattice for the proton, and the electron ring

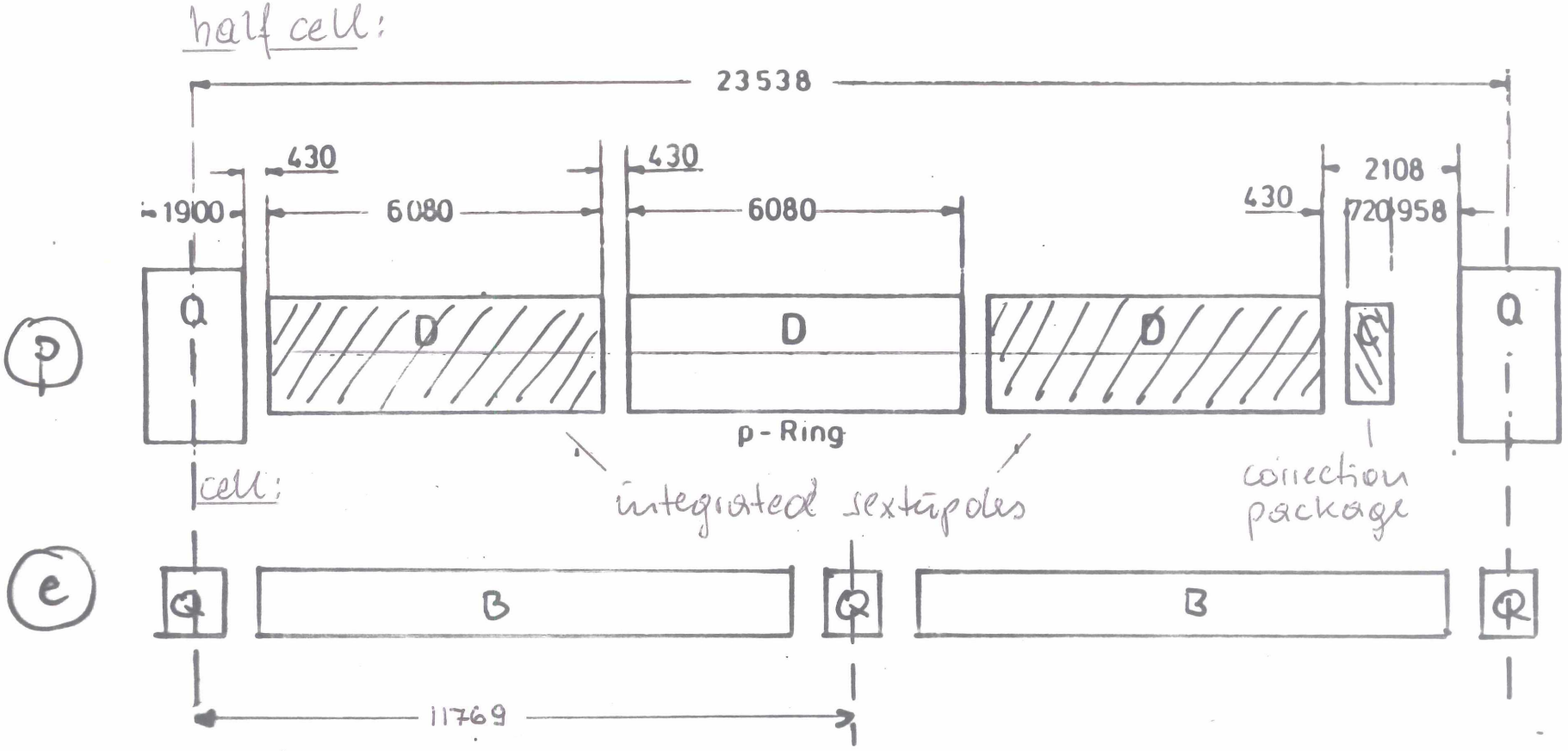


104 proton cells, 208 electron cells

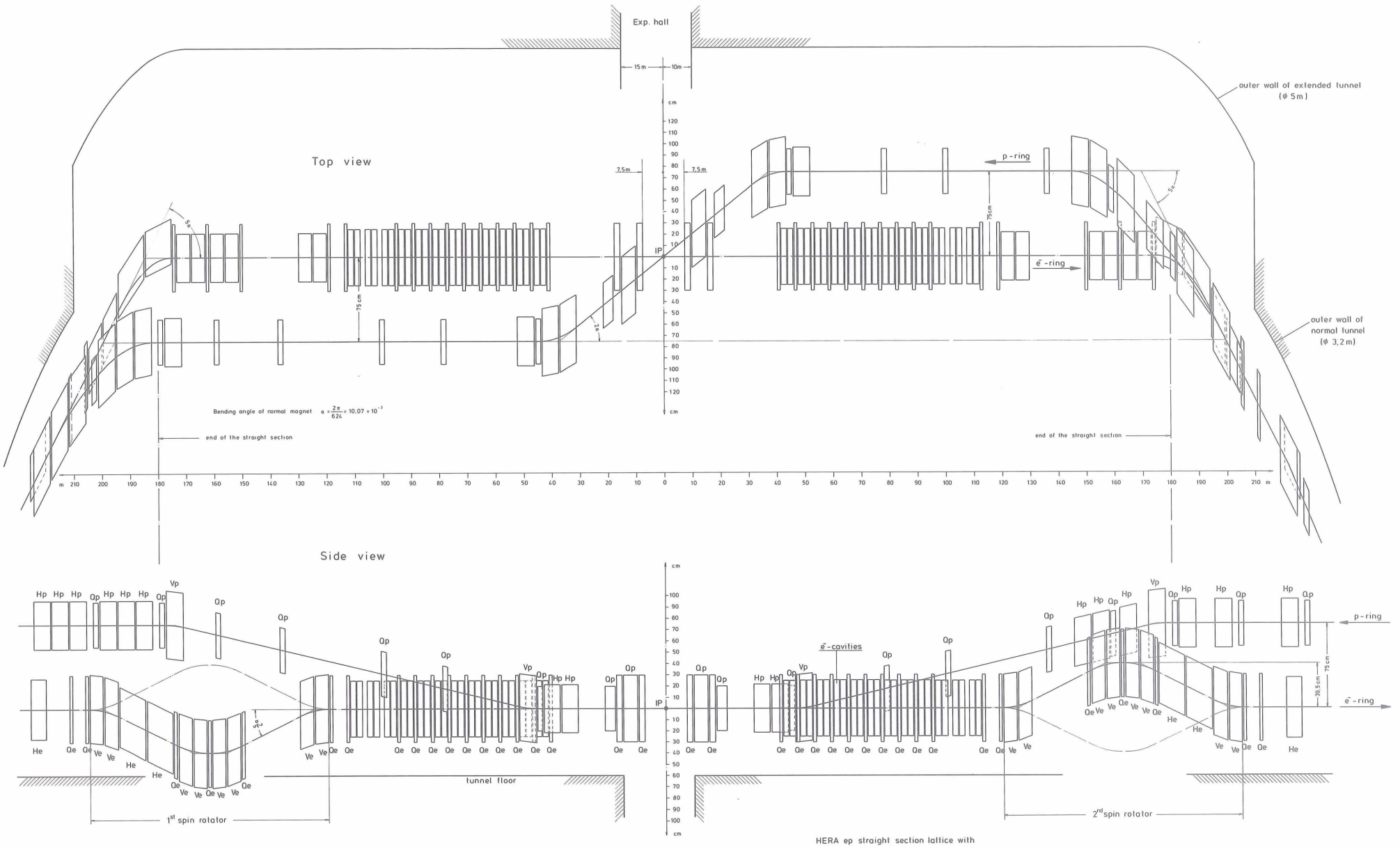


HERA ep straight section lattice with
interaction region and spin rotators

24. 3 1981
G Meyer , C Schulz
-MHC-

Fig.5: Layout of the interaction region

Fig.7: HERA - electron ring

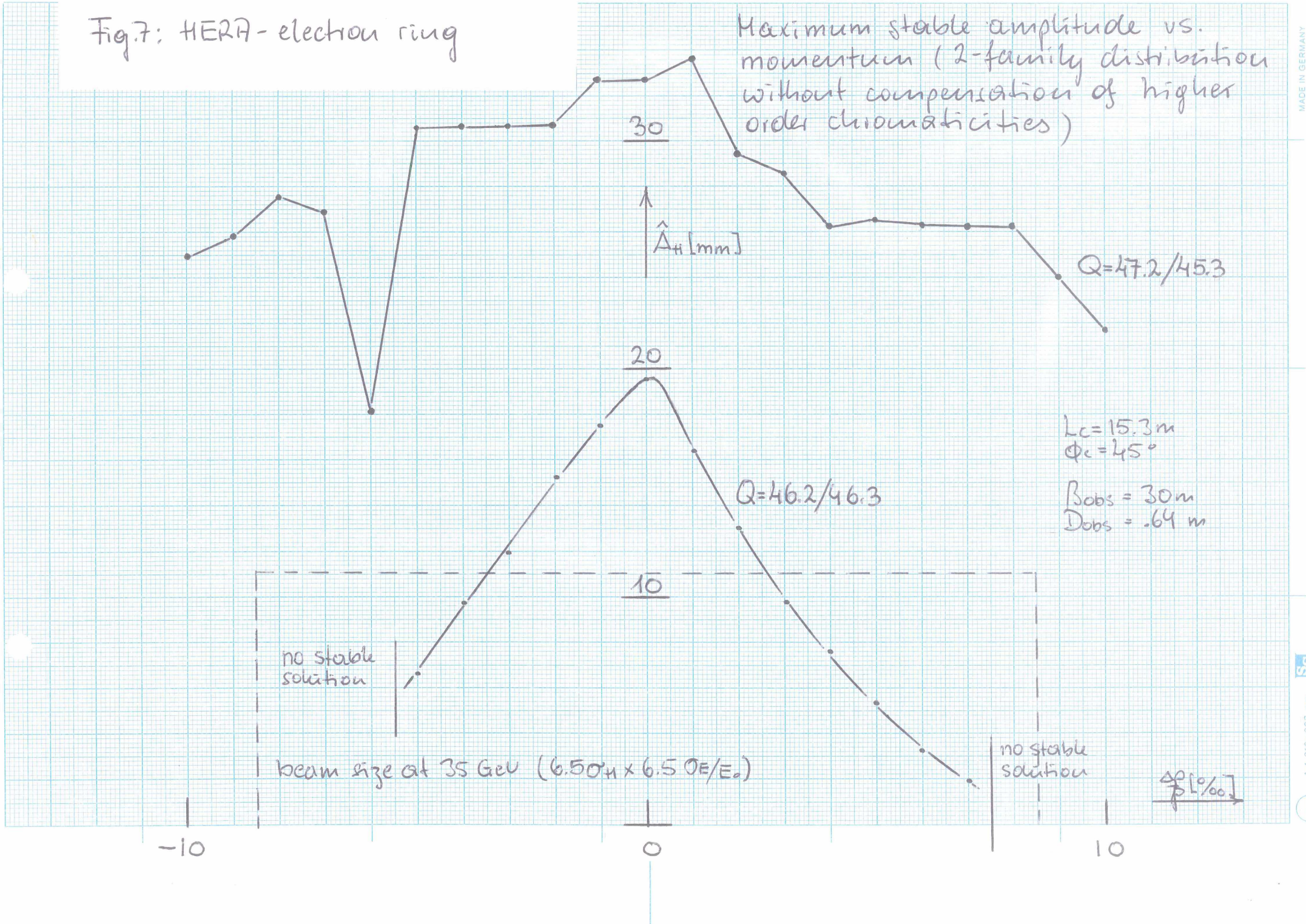

Fig.9 **HERA90 - tune variation**

Maximum stable initial amplitude vs. tune

rectangular beam
sextupoles only $\xi_{H,V} \approx 0$
emittance ratio $K = 0.5$
energy deviation $\Delta p/p = 0$
$Q_H = 33 + \delta Q_H \,/\, Q_V = 35 + \delta Q_V$
$N_{rev} = 100$

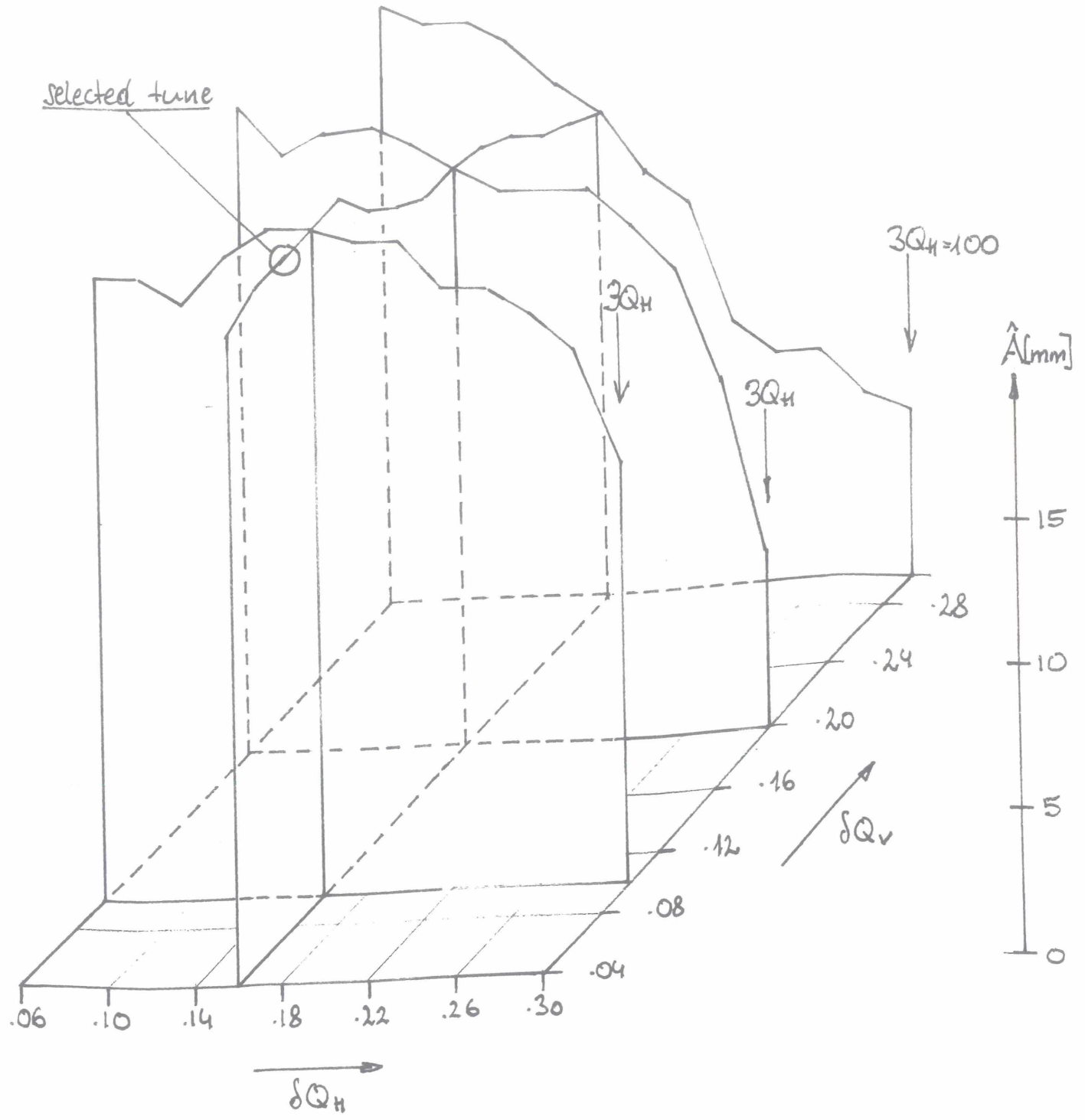

Fig. 8: HERA-electron ring
Tune variation with momentum

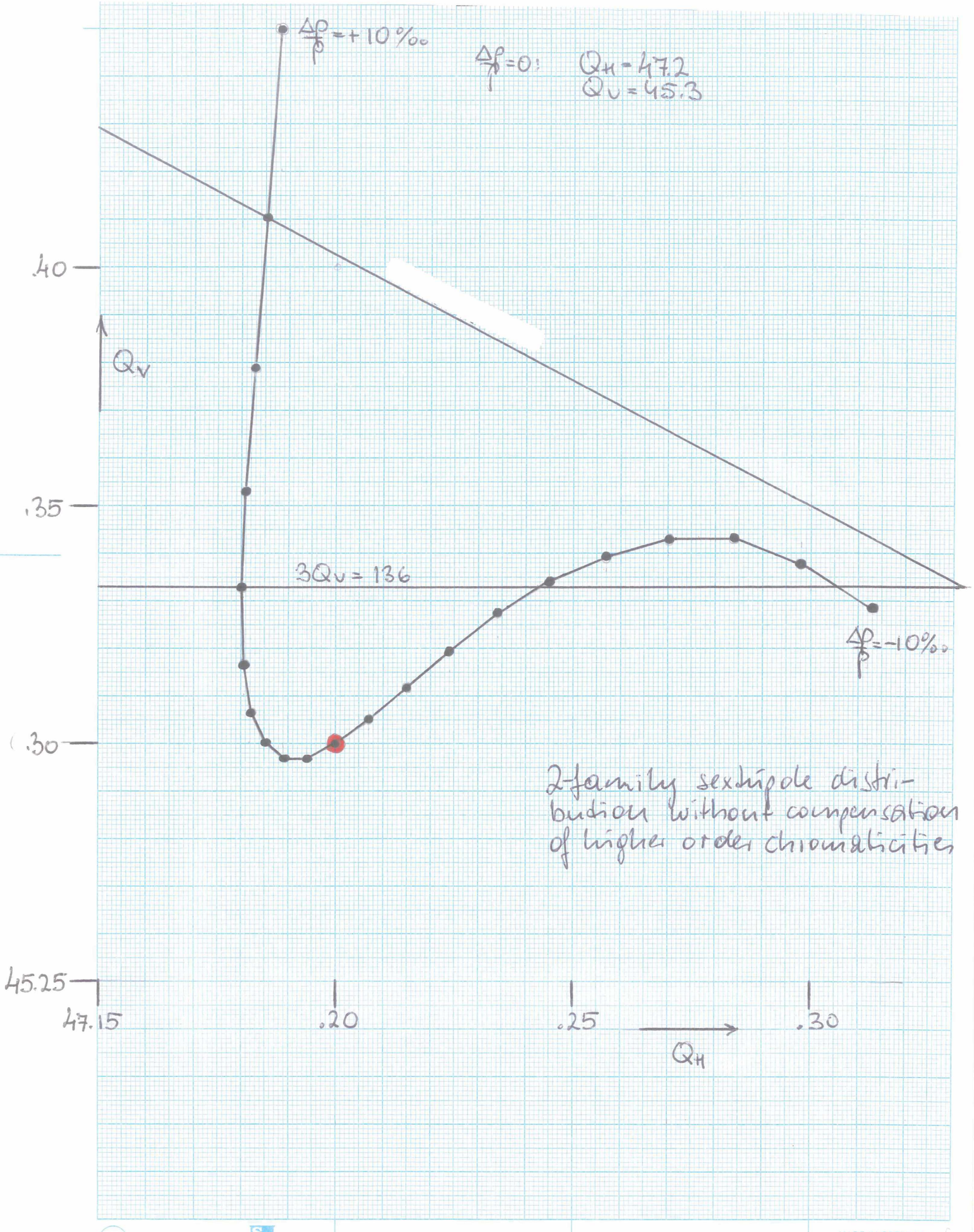

Fig.10 **HERA 90 - energydependence of tunes**

sextupoles only $\xi_{H,V} \approx 0$
$Q_H = 33.15$ } $\frac{\Delta p}{p} = 0$
$Q_V = 35.08$ }

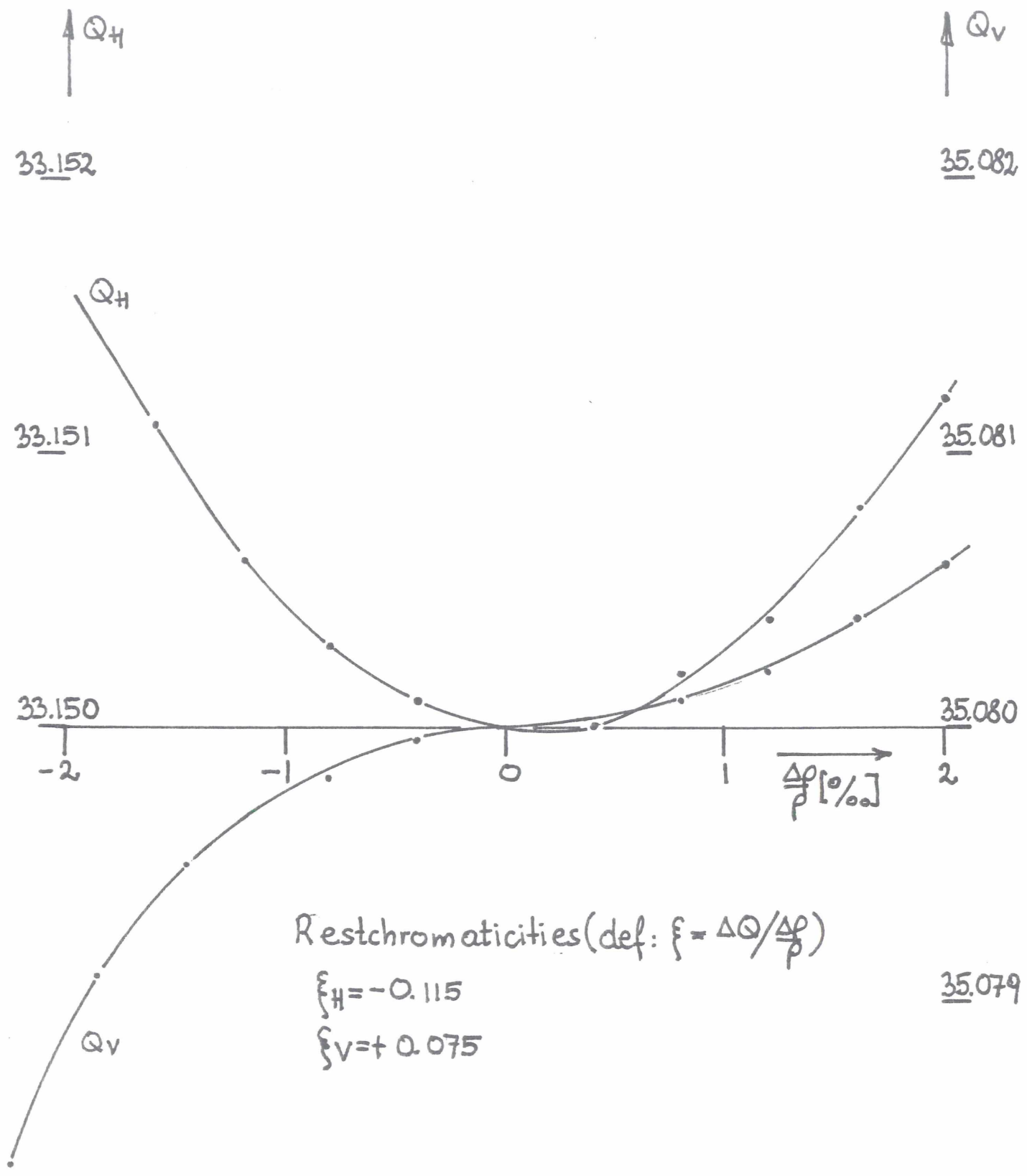


Restchromaticities (def: $\xi = \Delta Q / \frac{\Delta p}{p}$)

$\xi_H = -0.115$

$\xi_V = +0.075$

Fig.11: **HERA90 - energy variation**

Maximum stable initial amplitude vs. energy deviation

rectangular beam, sextupoles only, emittance ratio $\xi_{H,V} = 0$, $K = 0.5$

$Q_H = 33.15$ / $Q_V = 35.08$

$N_{rev} = 100$

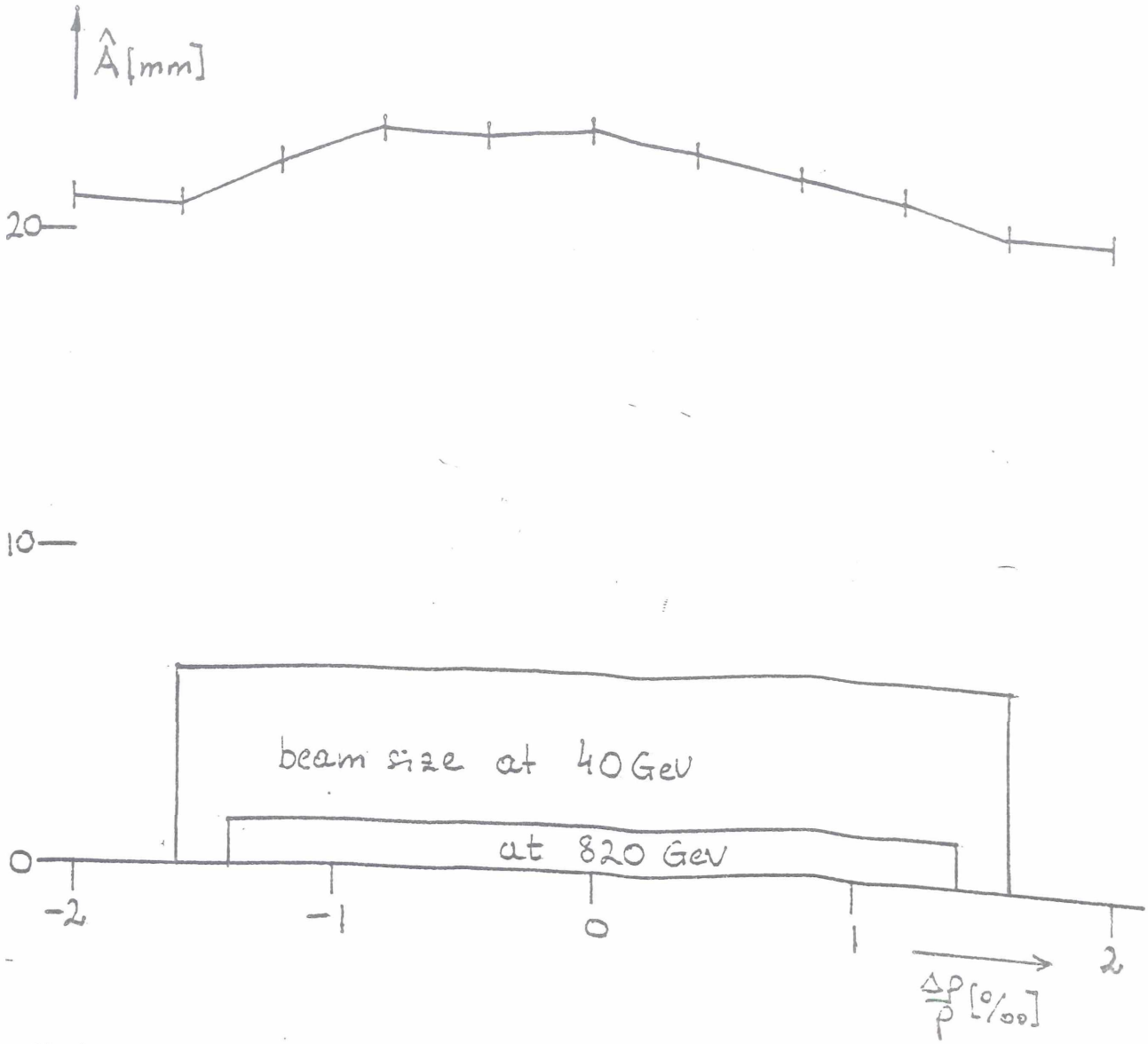


Definitions:

Maximum stable initial amplitude $\hat{A} = \hat{a}\sqrt{\frac{\beta_H(\frac{\Delta p}{p}=0)}{\beta_H(\frac{\Delta p}{p}\neq 0)}}$

($\hat{a}$ ... tracking result for maximum stable initial amplitude at the observation point, $\beta_H = 76$ m, $\beta_V = 14.3$ m)

Beam size = $2.2\sigma_H$ * total energy spread

40 GeV: $\varepsilon_H = 0.1$ $\pi$ mradmm ; $(\frac{\Delta p}{p})_{tot} = \pm 1.6$ ‰

820 GeV: $\varepsilon_H = 0.0047$ -"- ; -"- $= \pm 1.4$ ‰

Fig. 6

Fig. 12: HERA90 - number of stable revolutions vs. initial amplitude

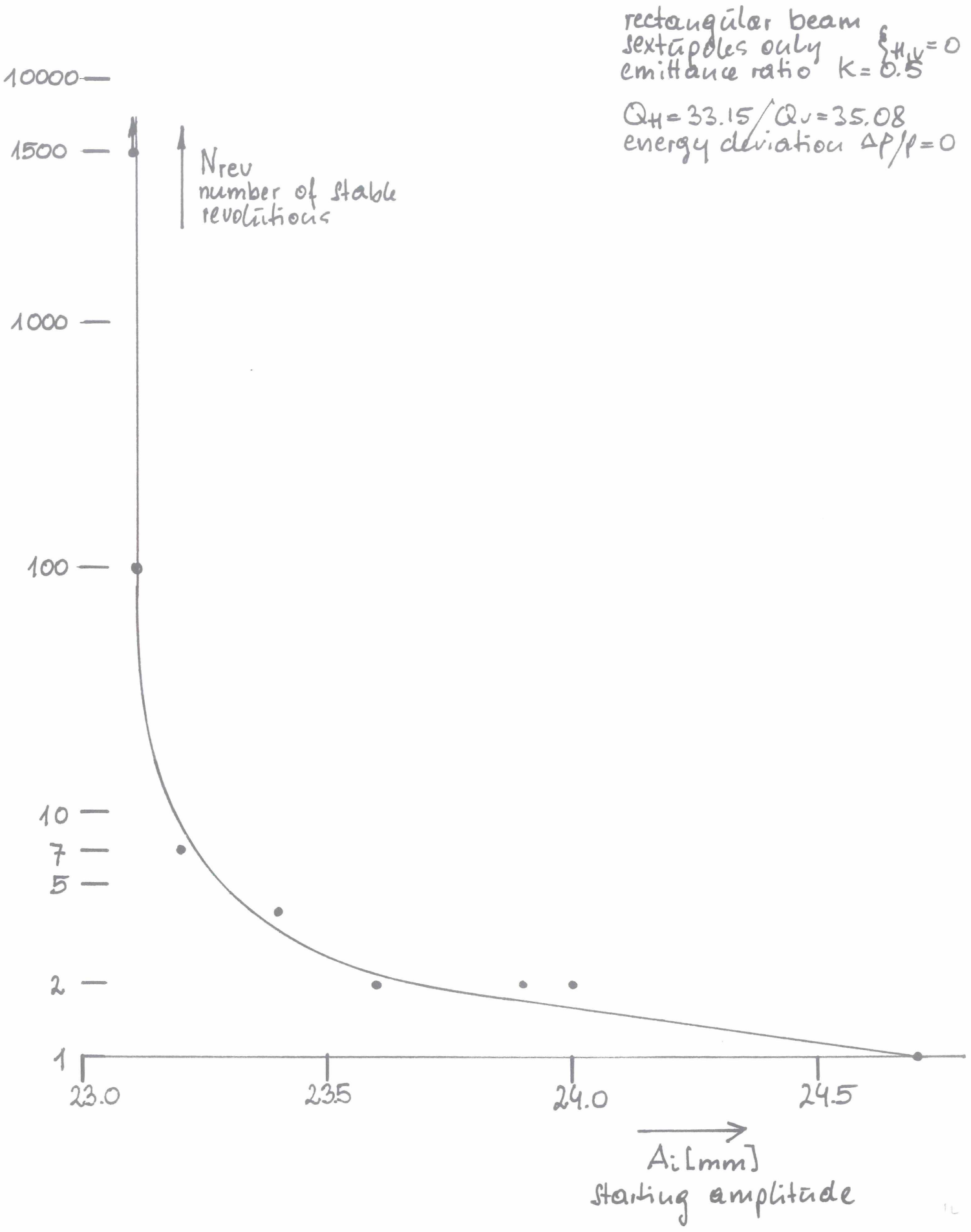


Fig 3

Fig. 13:

**HERA90/60 - aperture variation**

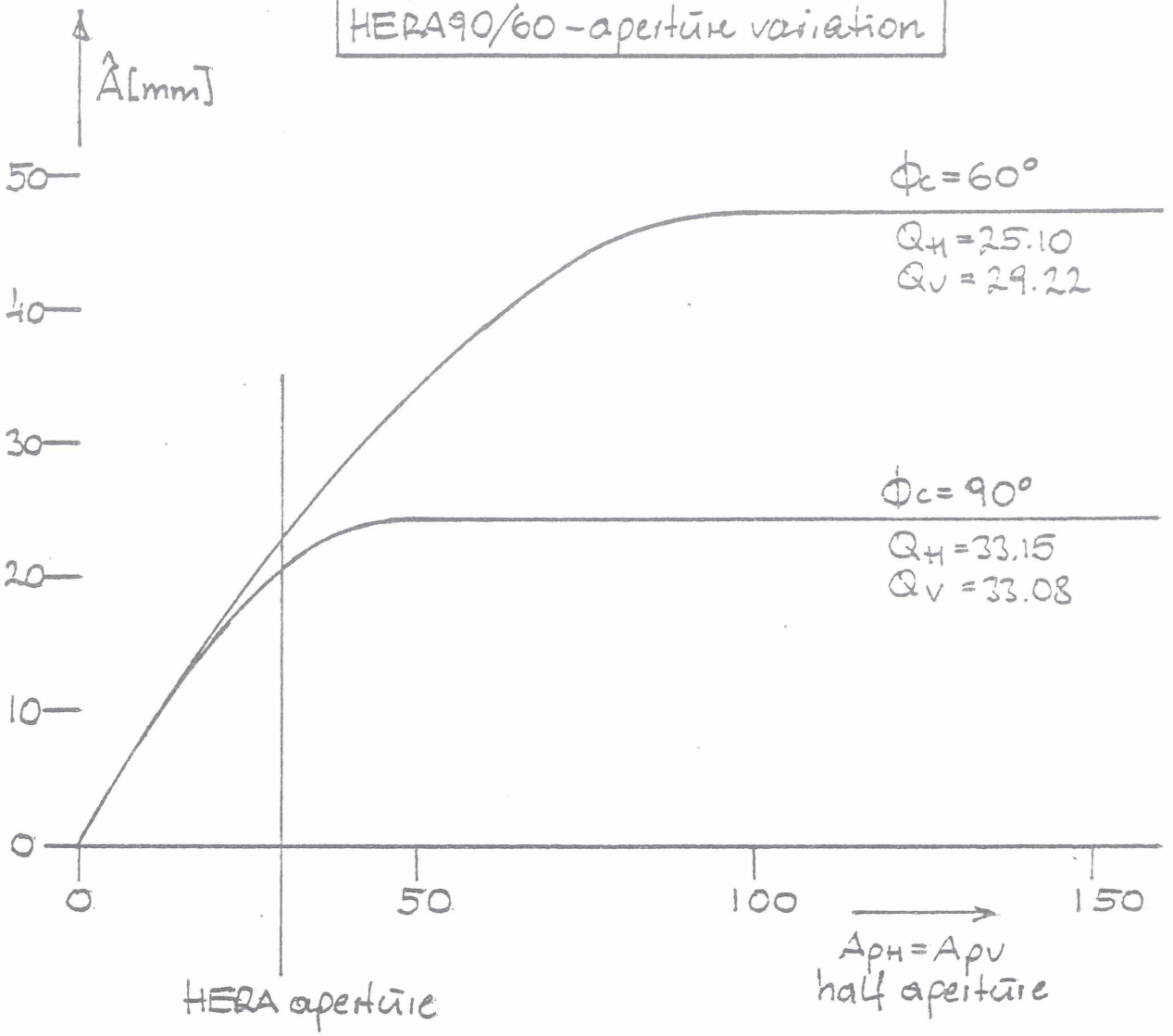


rectangular beam
sextupoles only
emittance ratio K=1.0
no energy deviation

Niev = 30 !

HERA90 – Variation of maximum stable amplitude with multipole statistics

Fig. 14

rectangular beam
sextapoles and multipoles $\{_{H,V}=0$
with closed orbit errors c.o.-rms = 1 mm
emittance ratio $K = 0.5$
energy deviation $\Delta p/p = 0$
$N_{RCU} = 100$

A: $Q_H = 33.15 / Q_V = 35.18$

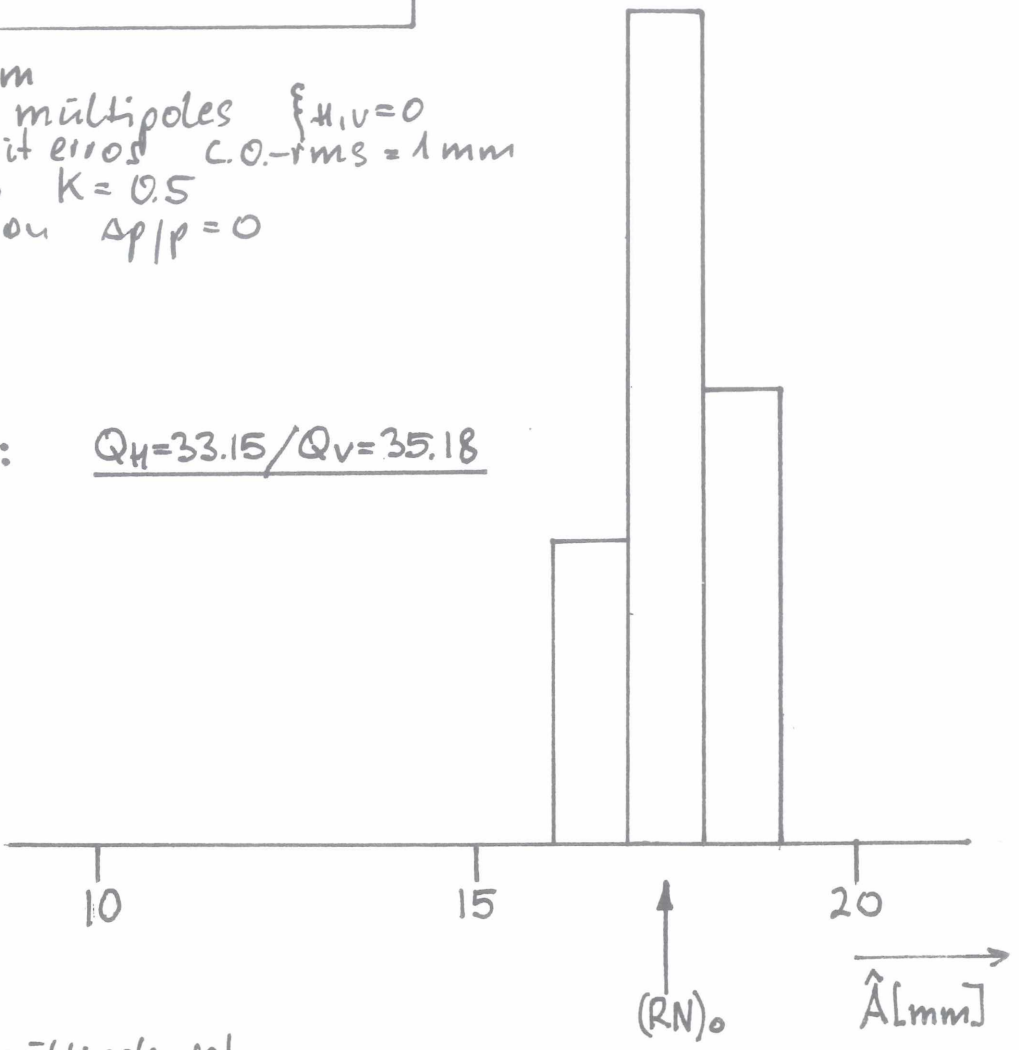


$(RN)_0$ = random multipole set selected for proceeding calculations

B: $Q_H = 33.15 / Q_V = 35.08$

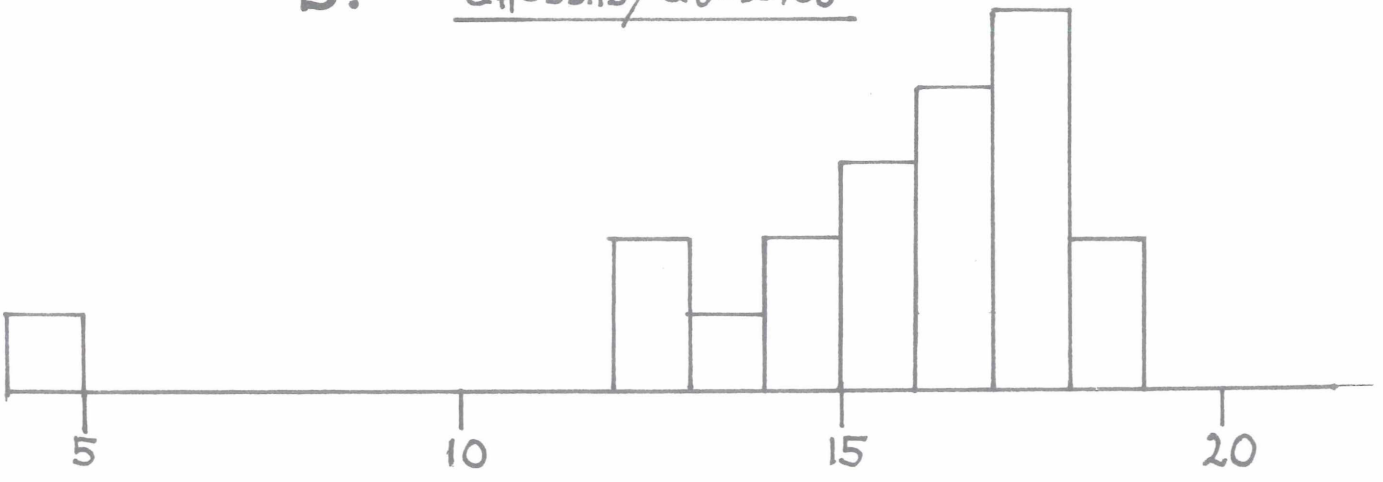

Fig. 15: **HERA 90 - energy variation**

Maximum stable initial amplitude vs. energy deviation

rectangular beam
sextupoles and multipoles
emittance ratio $K = 0.5$
$Q_H = 33.15 / Q_V = 33.18$
$N_{IEV} = 100$
orbit rms-error = 1 mm

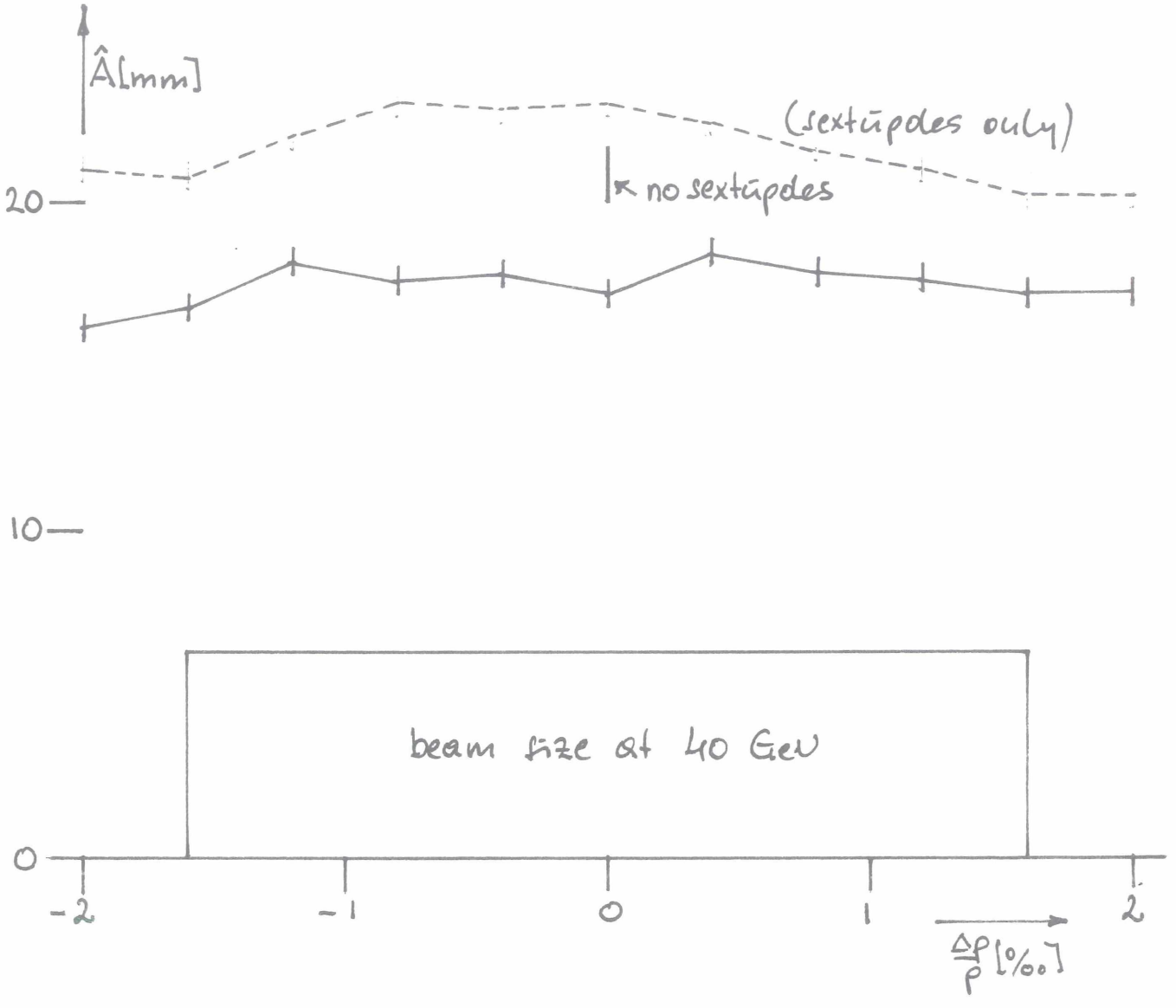

Fig. 16: HERA-proton ring ($\phi_c = 90°$)
Maximum stable amplitude vs. tune, before 3rd integer resonance compensation (see Ref. /6/)

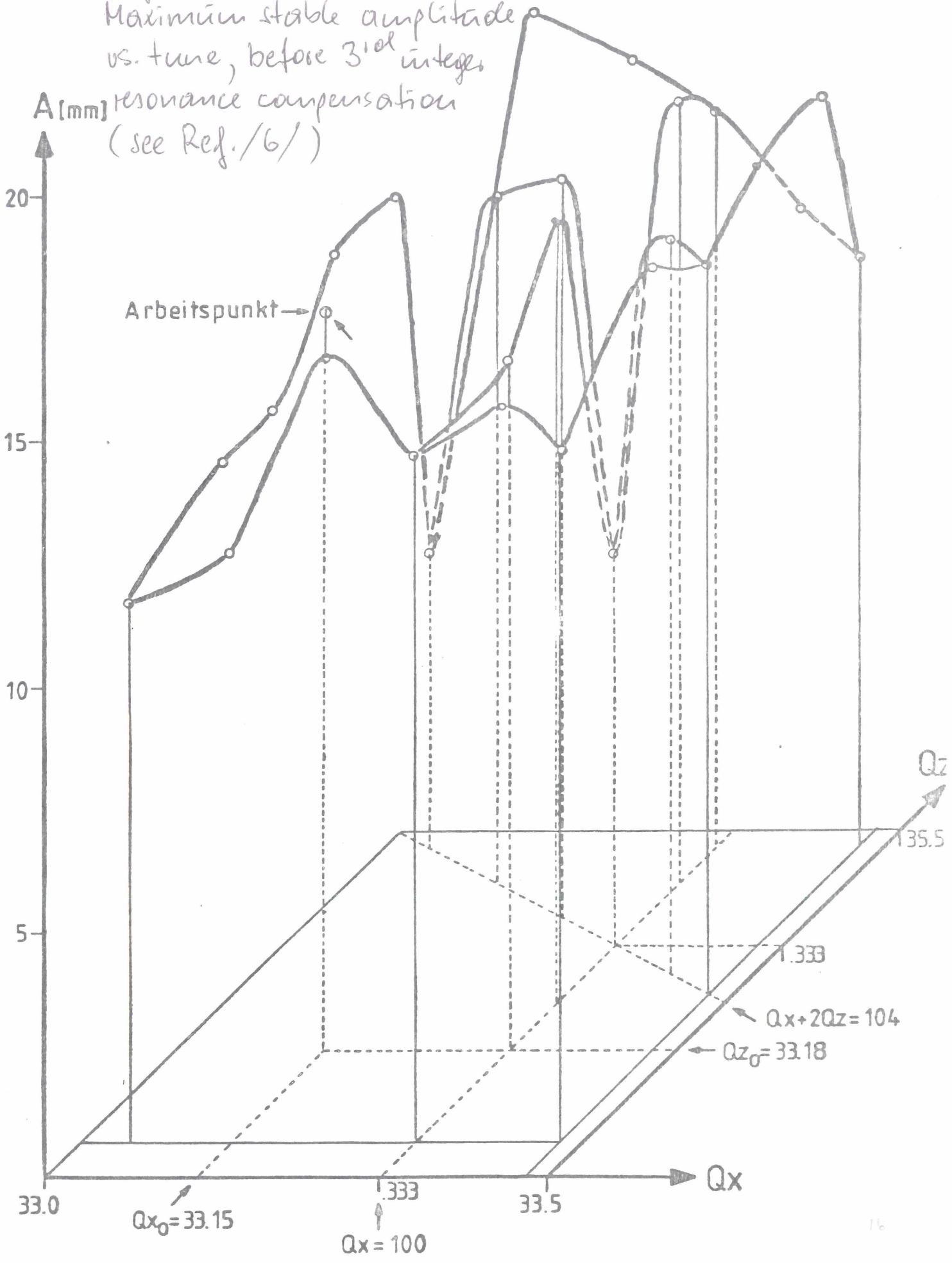

Fig. 17: HERA – proton ring ($\varphi_c = 90°$)
Maximum stable amplitude vs. tune, after 3rd integer resonance compensation (see Ref. /6/)

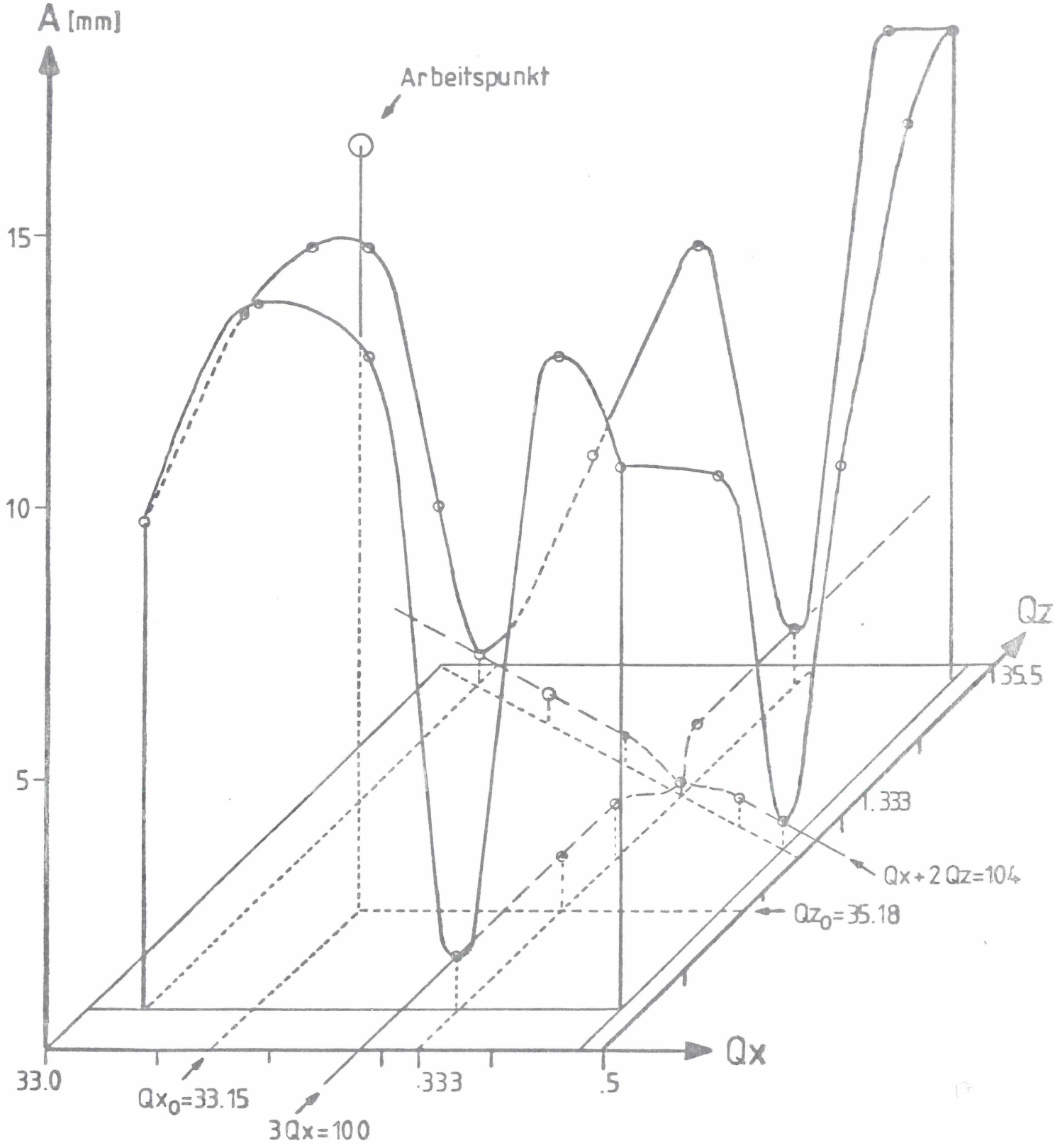

Fig. 18: **HERA90 – 14 and 18 pol mean value variation**

rectangular beam
no sextupoles
no multipoles
no orbit ellipse
$N_{iso} = 30$
$\Delta p = 0$

$Q_H = 23.15$
$Q_v = 25.18$

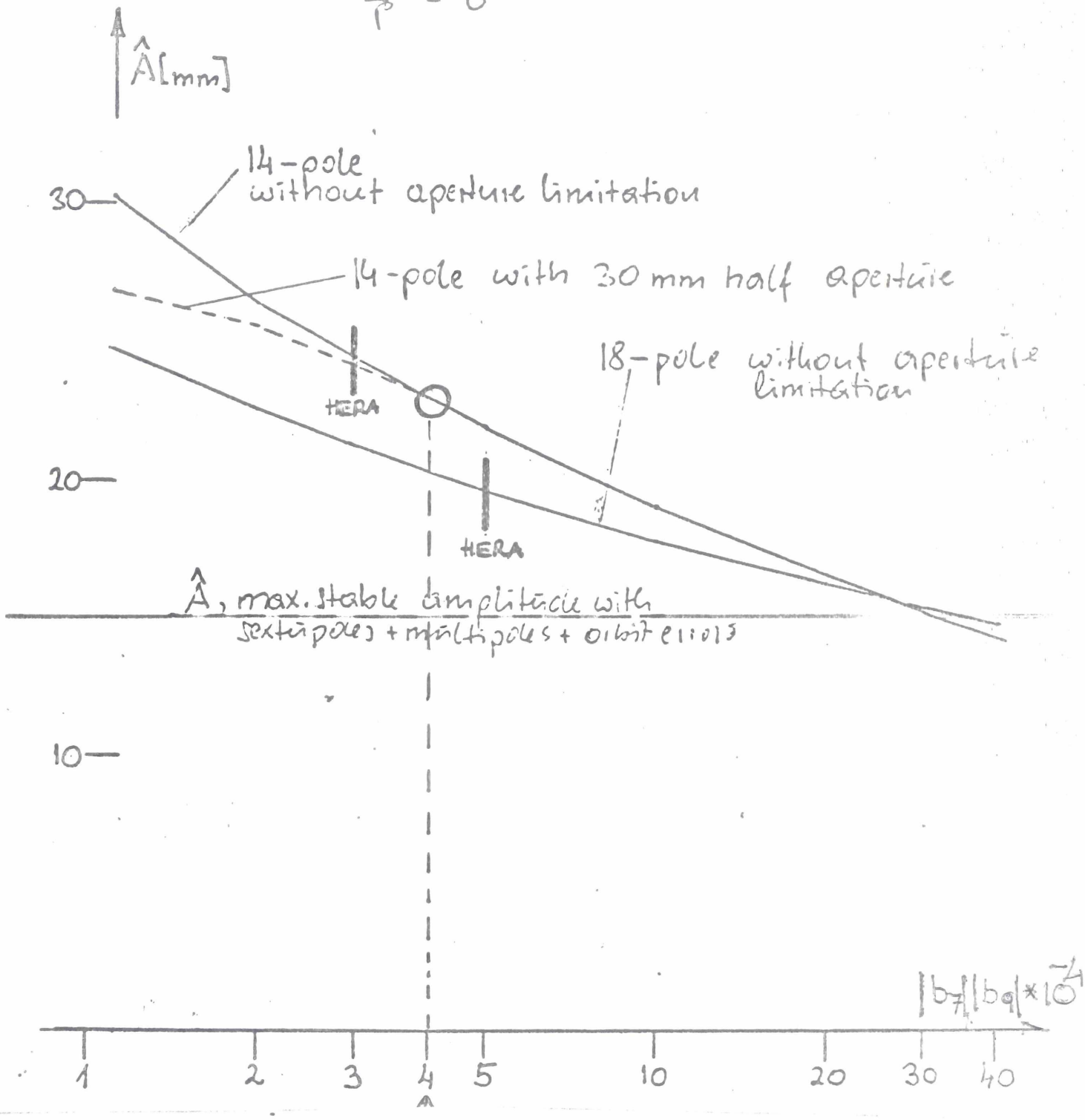

Fig. 23: HERA-proton ring ($\phi_c = 90°$)
Variation of stable amplitude with aperture

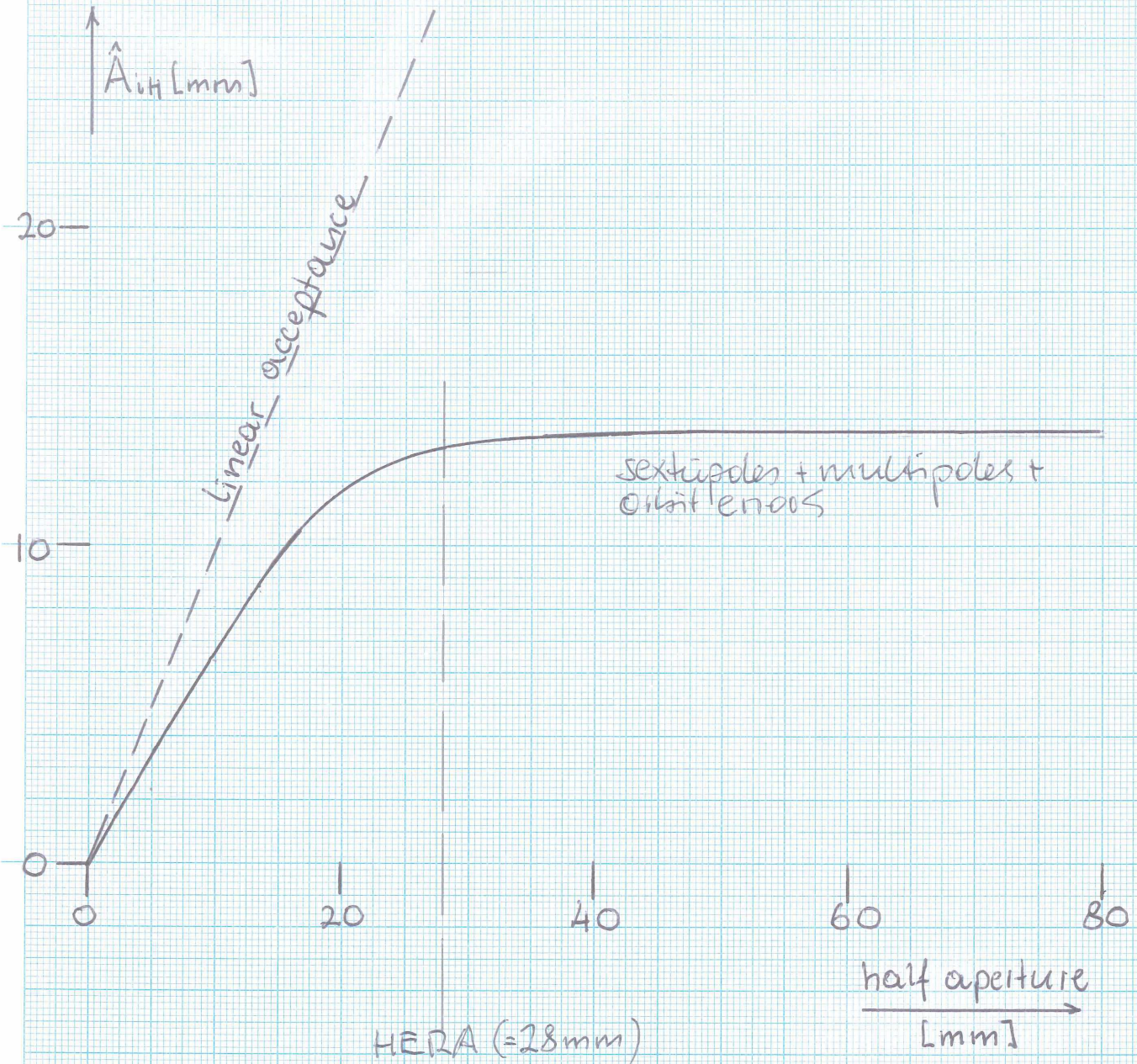

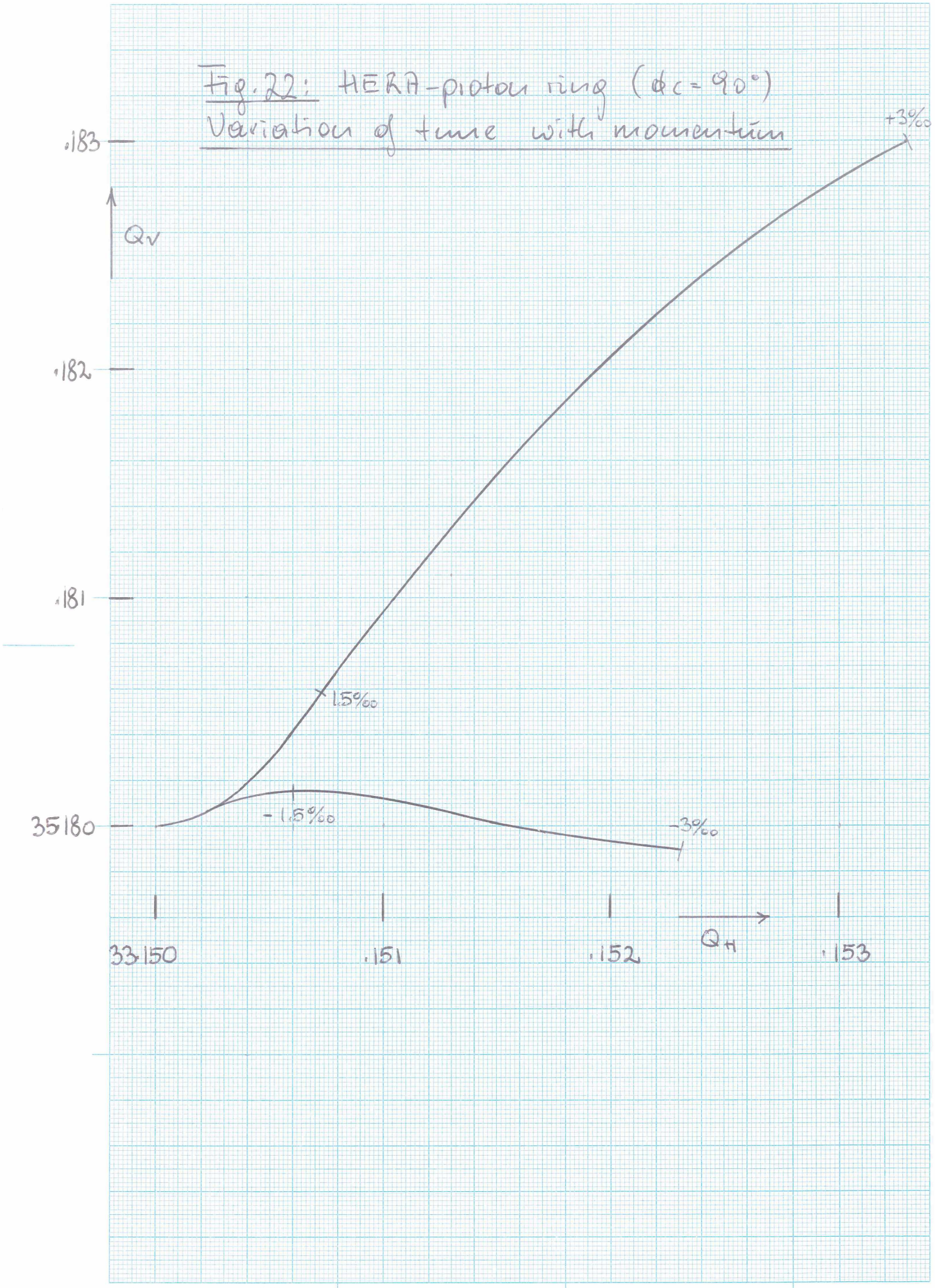

Fig. 19: HERA 90 – maximum amplitude vs. momentum deviation with persistent sextupole compensated by normal lattice sextupoles

rectangular beam
sextupoles + multipoles
1mm orbit, rms errors
emittance ratio $K = 1.0$

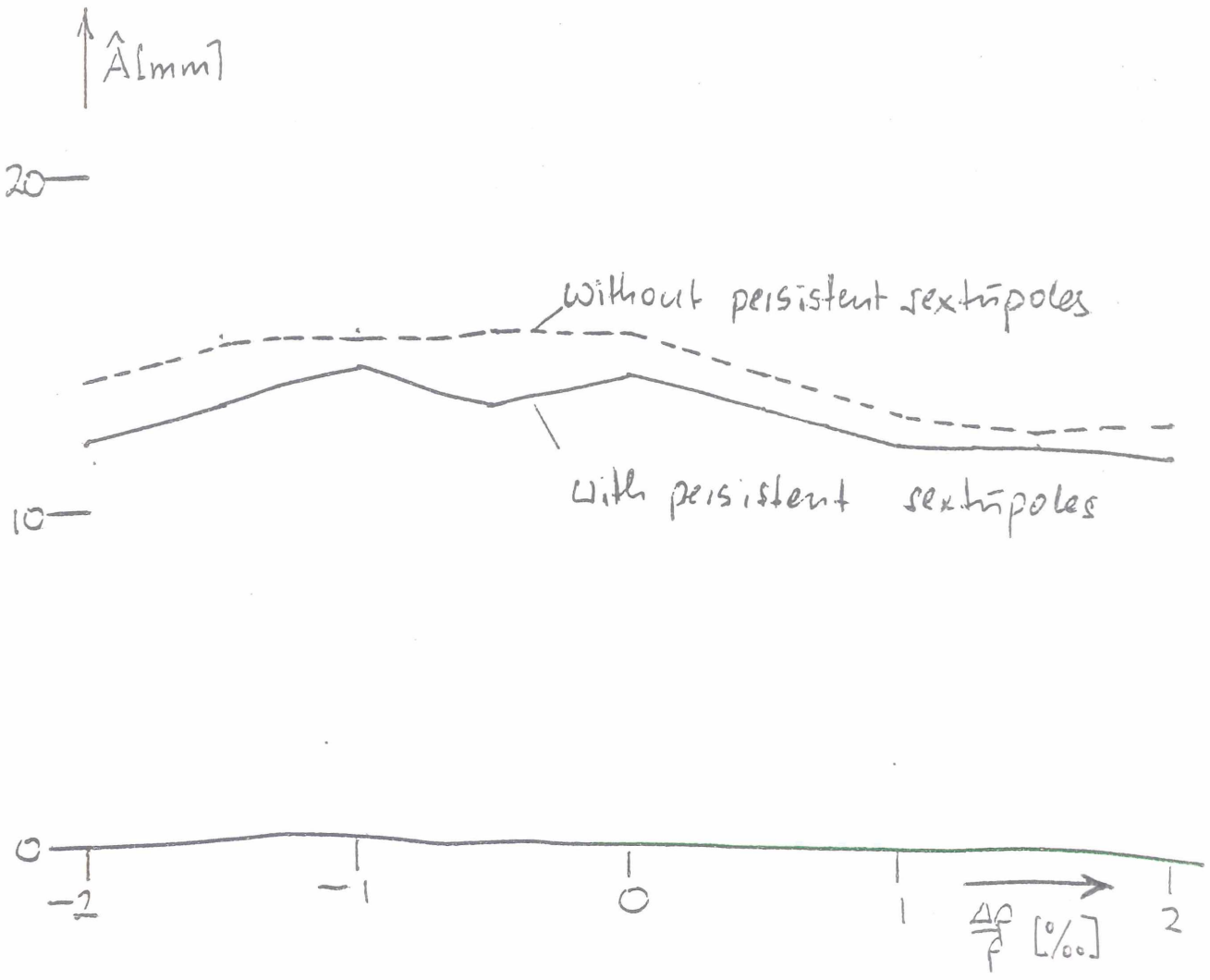

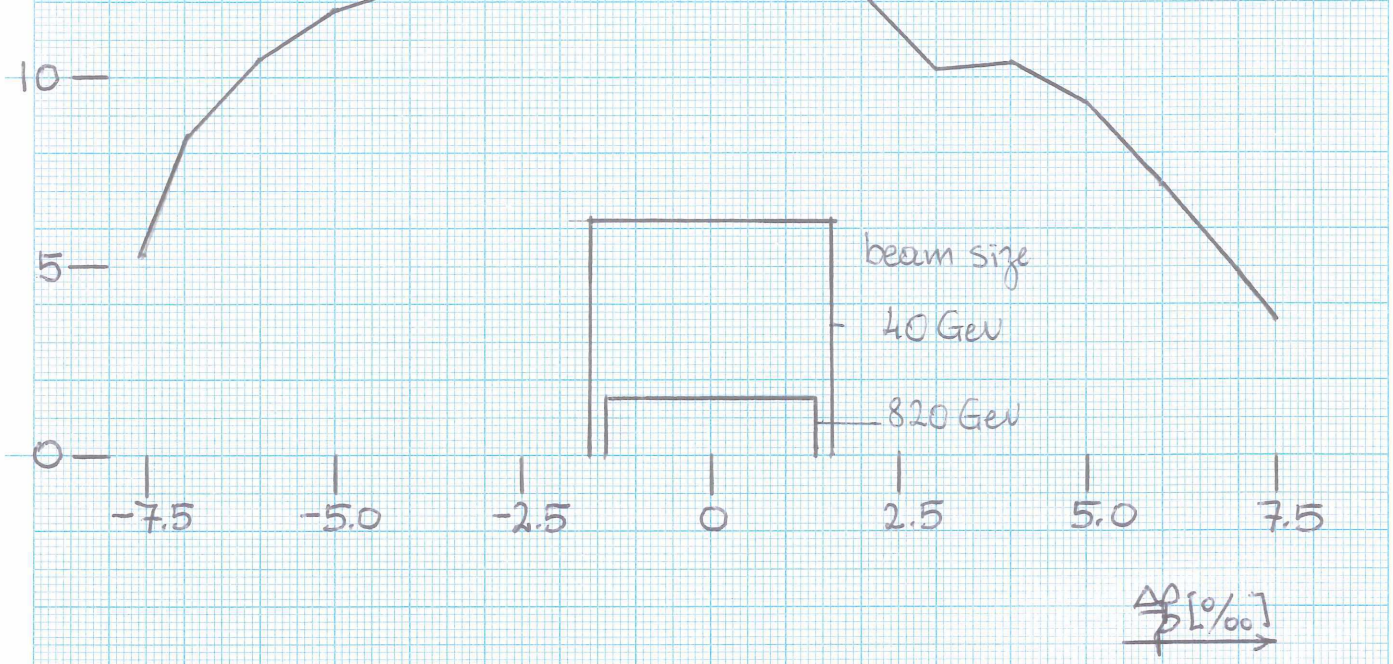

Fig. 21: HERA-proton ring ($\phi_c = 90°$)
Stable energy range

PCS compensated by integrated sextupoles

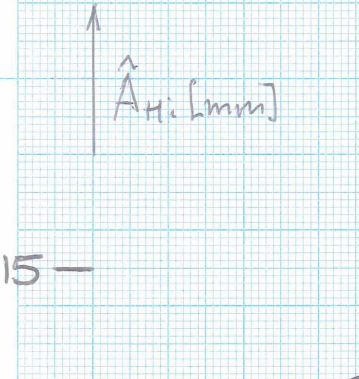

Fig. 20: HERA-proton ring ($\phi_c = 90°$)
Maximum stable amplitude vs. momentum, with PCS compensated by sextupoles integrated in the bending magnets adjacent to the lattice quadrupoles

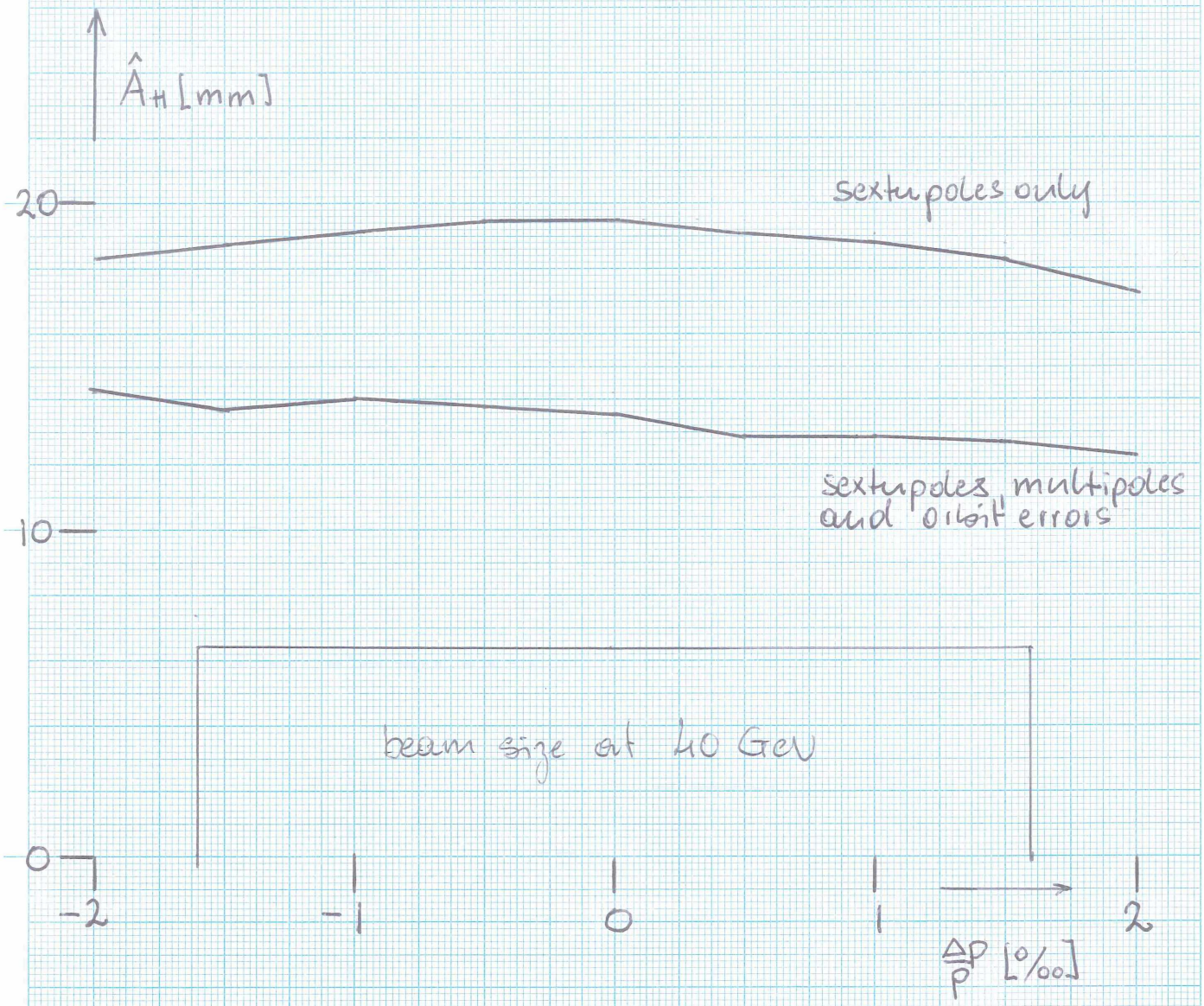


16 particels
100 revolutions
1mm orbit rms error
$Q_H = 33.15$ / $Q_V = 35.18$
$K = 1.0$
$\xi_H = \xi_V = 0$

Fig. 24: HERA-proton ring ($\phi_c = 90°$)
Variation of stable amplitude with PCS

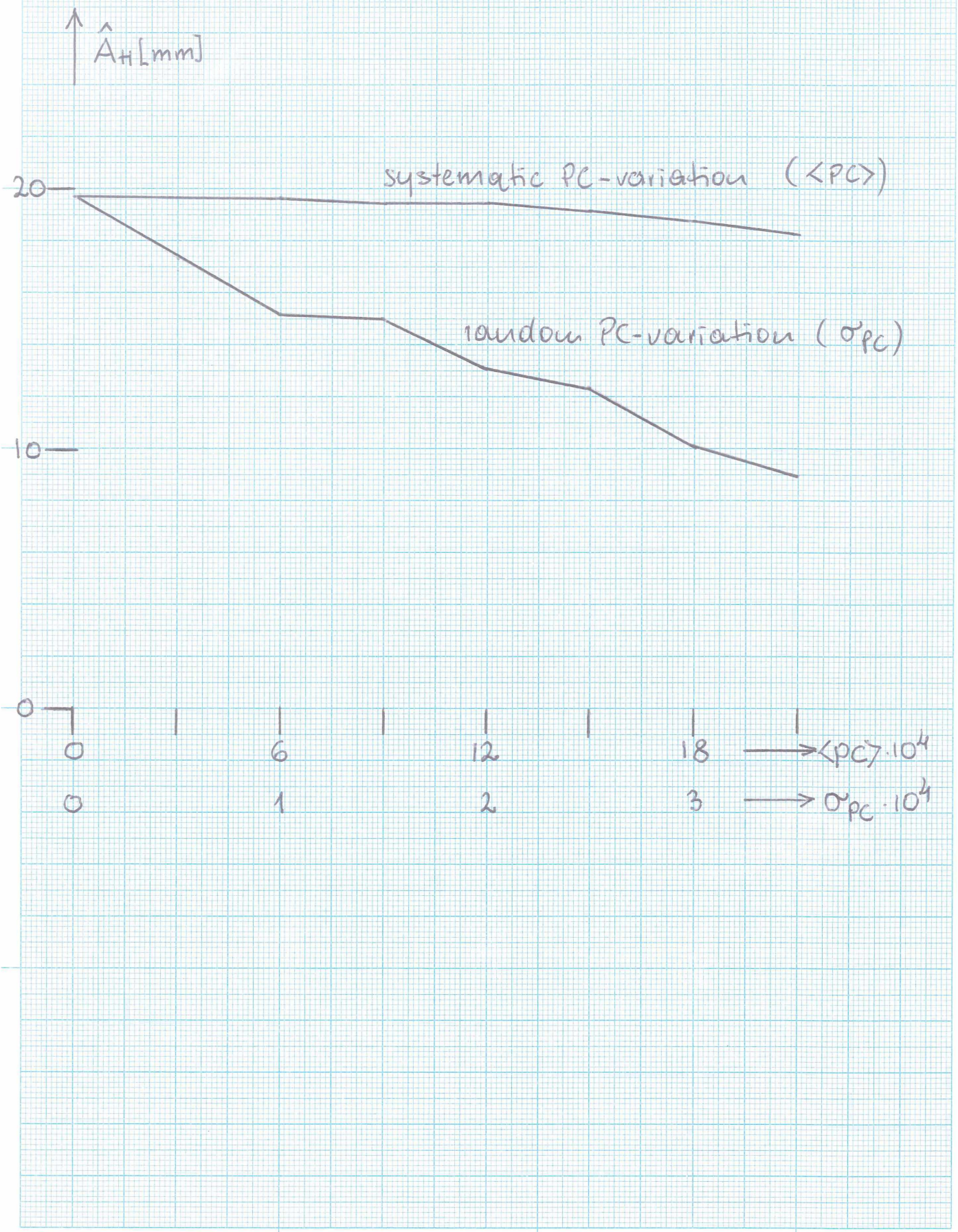

Fig. 25: HERA - proton ring ($\phi_c = 90°$)
Maximum stable amplitude with increasing orbit distortions

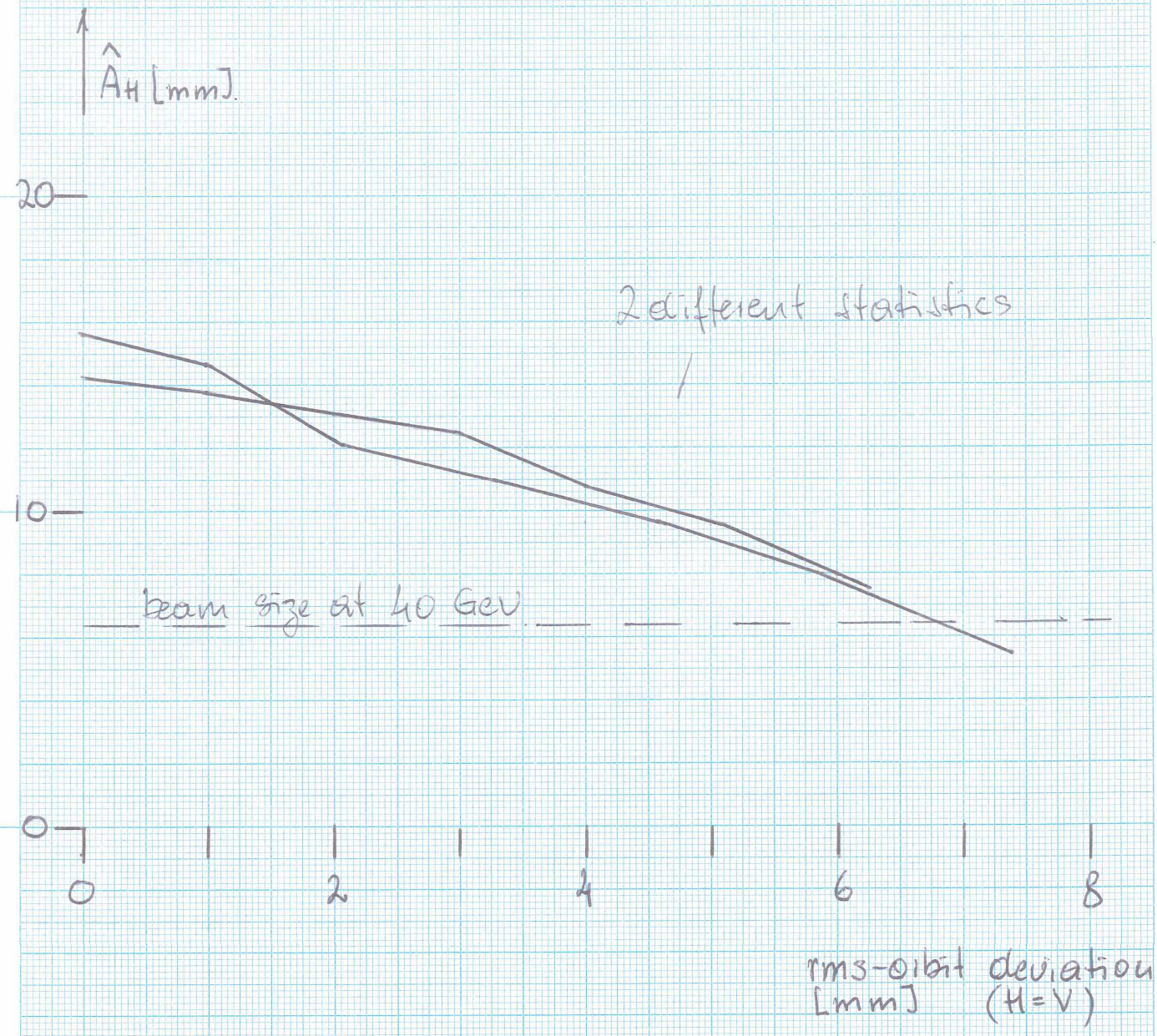


16 particles
100 revolutions
$Q_H = 33.15$ / $Q_V = 35.18$
$\xi_H = \xi_V = 0$
tunes readjusted
chromaticities compensated

Fig. 26: HERA-proton ring ($\varphi_c = 90°$)
Number of stable revolutions vs. initial amplitude

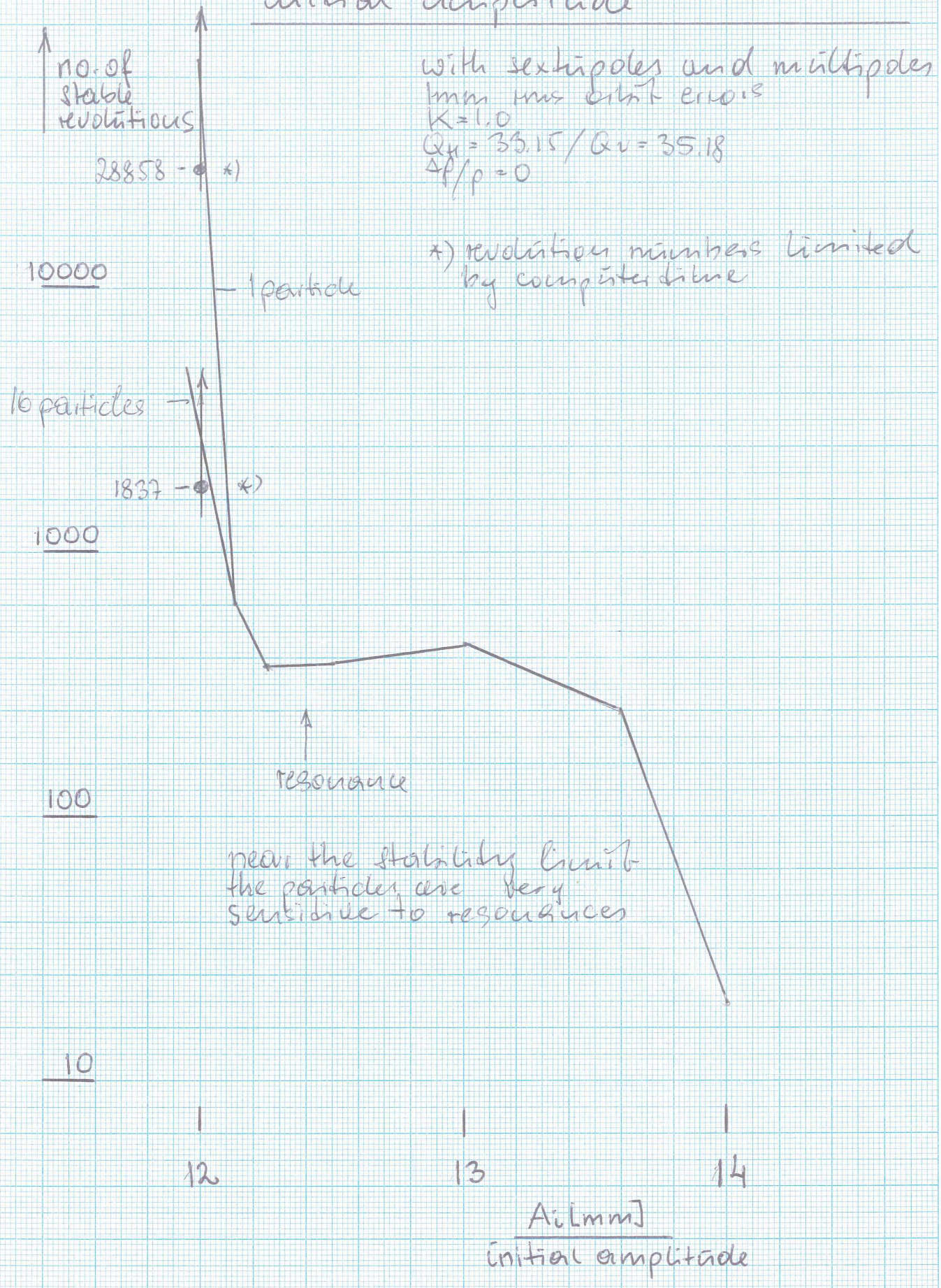


with sextupoles and multipoles
1mm rms orbit errors
$K = 1.0$
$Q_H = 35.15 / Q_V = 35.18$
$\Delta p/p = 0$

*) revolution numbers limited by computer time